Presented at the Plenary Session of the
12th International Workshop on the Physics of Compressible Turbulent Mixing
Moscow, Russian Federation

Rayleigh–Taylor Turbulent Mixing: Synergy Between Simulations, Experiments, and Modeling

15 July 2010

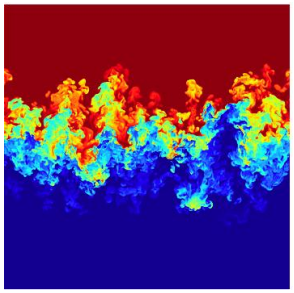

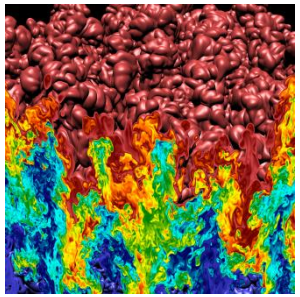

Oleg Schilling†

Lawrence Livermore National Laboratory

†in collaboration with Nicholas J. Mueschke, Gregory C. Burton, and Malcolm J. Andrews

Lawrence Livermore National Laboratory, P.O. Box 808, Livermore, CA 94551

This work was performed under the auspices of the U.S. Department of Energy by Lawrence Livermore National Laboratory under Contract DE-AC52-07NA27344

LLNL-PRES-439132

DNS data was used to examine exact and modeled turbulent transport equations and to develop closures for Rayleigh–Taylor mixing

- This work integrates DNS, experimental data, and modeling
- Measurements from a *Sc* = 7 water channel experiment used to initialize DNS
- Develop *a priori* optimized gradient-diffusion and similarity closures
  - Compute quantities in turbulent viscosity-based closures (K, ε, ν_t *etc.*)
  - *Compute model coefficients unavailable experimentally*
  - Show that many coefficients asymptote at late times
  - Demonstrate good correlation between modeled terms and DNS data across mixing layer using these dynamic coefficients
- Validate model *a posteriori* by comparison to DNS and experimental data for *Sc* = 7 mixing
- Extend model to *Sc* ~ 10^3 mixing and compare to experimental data

This work demonstrates the use of 3- and 4-equation turbulence models for Rayleigh–Taylor instability-induced mixing at different Schmidt numbers

The DNS[1] models a nonreacting water channel Rayleigh–Taylor mixing experiment[2] at Texas A&M

$L_x \times L_y \times L_z$	28.8 cm × 18 cm × 24 cm
$N_x \times N_y \times N_z$	1152 × 720 × 1280
A	7.5×10^{-4}
ρ_1	0.9986 g/cm^3
ρ_2	0.9970 g/cm^3
g	981 cm/s^2
Sc (Pr)	7.0

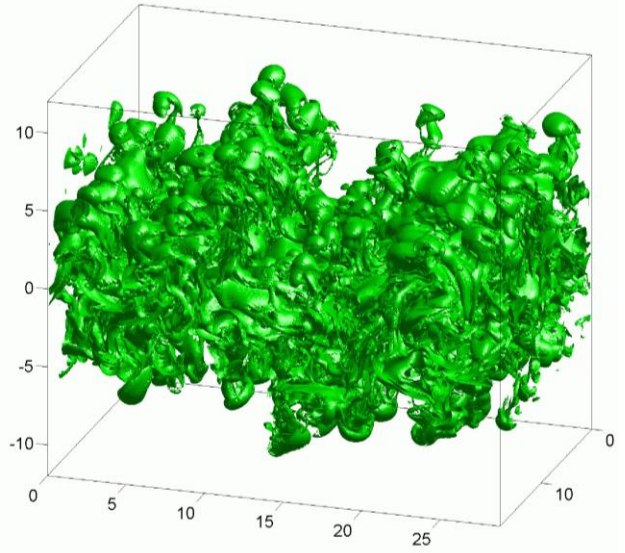

- **Initial velocity/interfacial perturbations taken from experimental data**
- **Time normalized by $\tau = t\sqrt{gA/H}$ (H = 32 cm is channel height)**
- **At latest time, integral-scale Reynolds number reaches ~ 4500**

[1] N. J. Mueschke, M. J. Andrews & O. Schilling, "Experimental characterization of initial conditions and spatio-temporal evolution of a small Atwood number Rayleigh–Taylor mixing layer," *J. Fluid Mech.* 567, 27 (2006)

[2] N. J. Mueschke & O. Schilling, "Investigation of Rayleigh–Taylor turbulence and mixing using direct numerical simulation with experimentally measured initial conditions. I. Comparison to experiment, II. Dynamics of transitional flow and mixing statistics ," *Phys. Fluids* 21, 014106, 014107 (2009a,b)

The initial velocity and interfacial perturbations were parameterized from experimental data

- **Interface perturbed in *x*- and *y*-directions** $\zeta(x,y) = \sum_{k_x} \hat{\zeta}_x \, e^{i\,k_x\,x} + \sum_{k_y} \hat{\zeta}_y \, e^{i\,k_y\,y}$
- **Velocity field constructed from perturbed potential field**

$$\phi_r(x,z) = \sum_{k_x} \frac{\hat{w}(k_x)}{k_x} \, e^{i\,k_x\,x} \, e^{-k_x\,|z|} \qquad u_i = \frac{\partial \phi_r}{\partial x_i} - \frac{D}{\rho}\frac{\partial \rho}{\partial x_i}$$

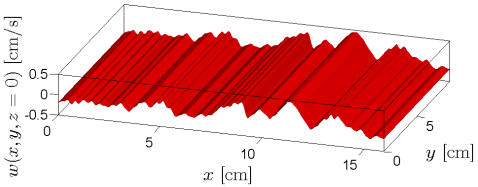

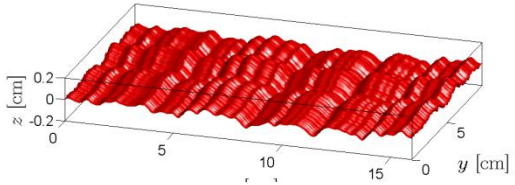

Initial density interface and vertical velocity at centerplane

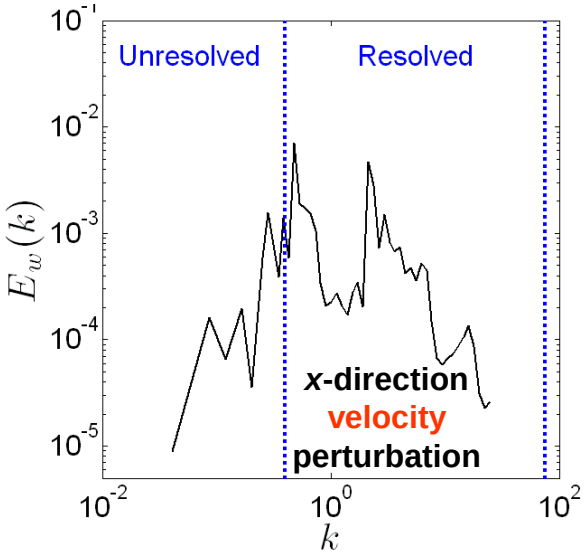

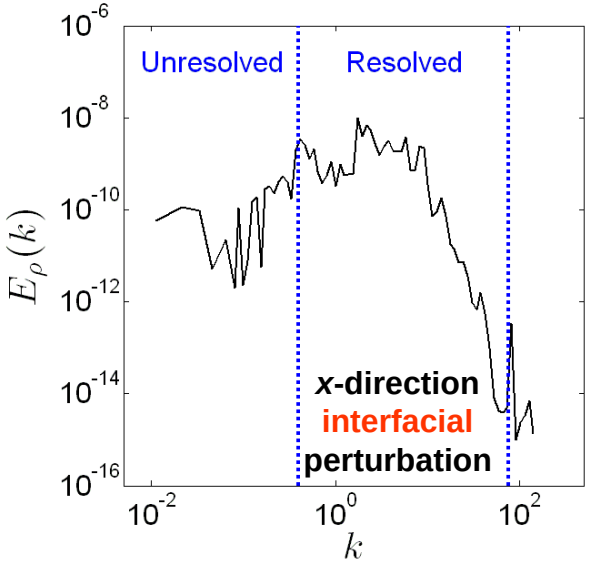

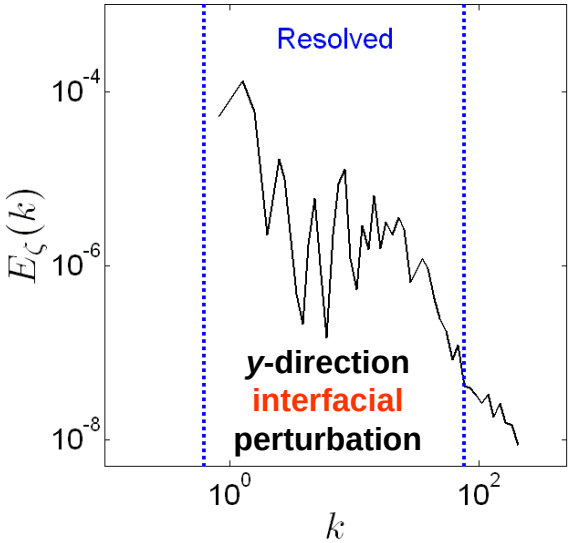

A spectral/10th-order compact difference and 3rd-order Adams–Bashforth–Moulton time-evolution scheme was used

- **Density, momentum, and mass fraction evolution equations**

$$\frac{\partial \rho}{\partial t} + \frac{\partial}{\partial x_j}(\rho\, u_j) = 0$$

$$\frac{\partial}{\partial t}(\rho\, u_i) + \frac{\partial}{\partial x_j}(\rho\, u_i\, u_j) = \rho\, g_i - \frac{\partial p}{\partial x_i} + \frac{\partial \sigma_{ij}}{\partial x_j}$$

$$\sigma_{ij} = \mu\left(\frac{\partial u_i}{\partial x_j} + \frac{\partial u_j}{\partial x_i}\right) - \frac{2}{3}\,\mu\,\delta_{ij}\,\frac{\partial u_k}{\partial x_k}$$

$$\frac{\partial}{\partial t}(\rho\, m_r) + \frac{\partial}{\partial x_j}(\rho\, m_r\, u_j) = \frac{\partial}{\partial x_j}\left(\rho\, D\,\frac{\partial m_r}{\partial x_j}\right)$$

where ρ, u_i, p, g_i, m_r, D, and σ_{ij} are the density, velocity, pressure, acceleration, mass fraction of fluid r, mass diffusivity, and the viscous stress tensor (μ is the dynamic viscosity)

Taylor's hypothesis related the temporal evolution of statistics to the spatial evolution

- $\Delta T \approx 5°$
- $A = 7.5 \times 10^{-4}$
- $U_m \approx 4.2$ cm/s mean velocity
- $Pr = 7$
- Downstream distance x from splitter plate related to time by

$$t = \frac{x}{U_m}$$

- Dimensionless time given by Boussinesq scaling

$$\tau = t\sqrt{\frac{g\,A}{H}} = \frac{x}{U_m}\sqrt{\frac{g\,A}{H}}$$

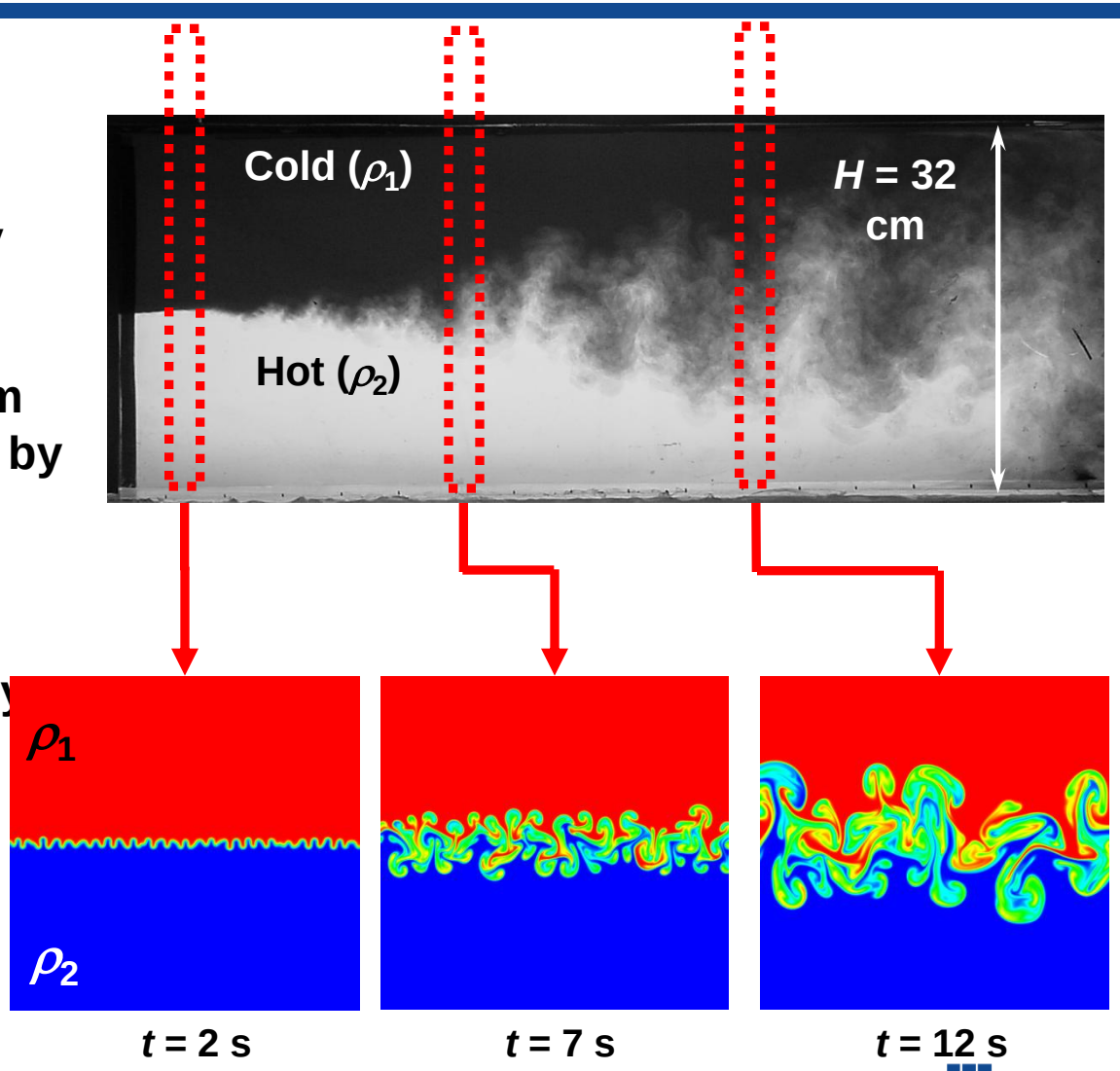

3D DNS visualizations show initially 2D behavior with 3D structure emerging at later times

τ = 0.15

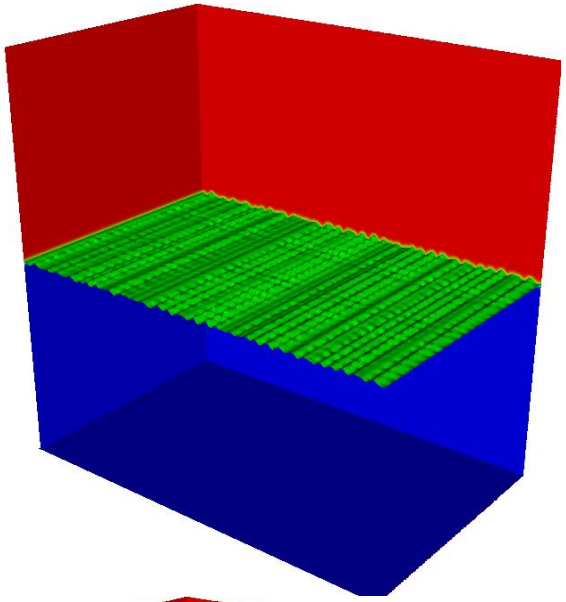

τ = 0.61

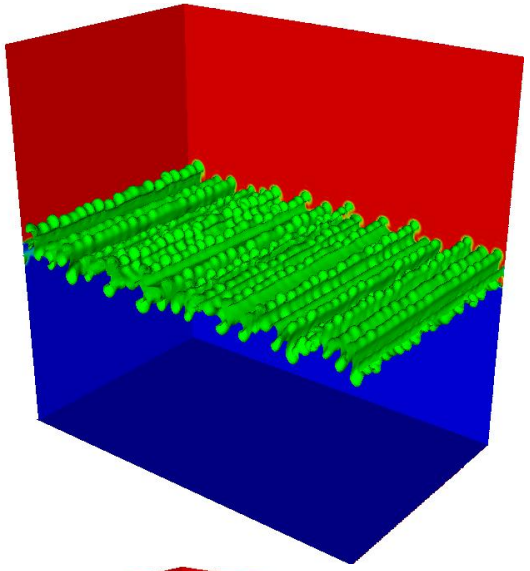

τ = 1.06

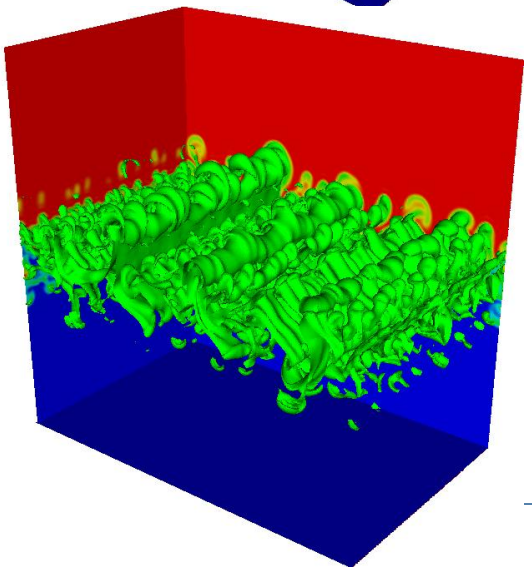

τ = 1.52

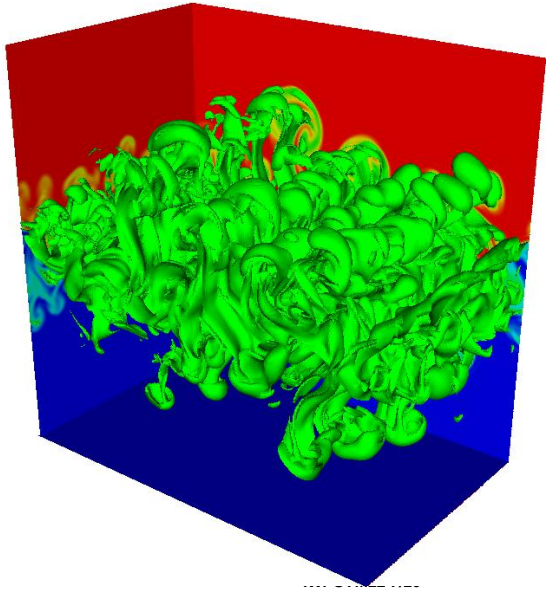

The centerplane density shows the transition from a nearly 2D initial state to a more 3D flow at late times

τ = 0.15

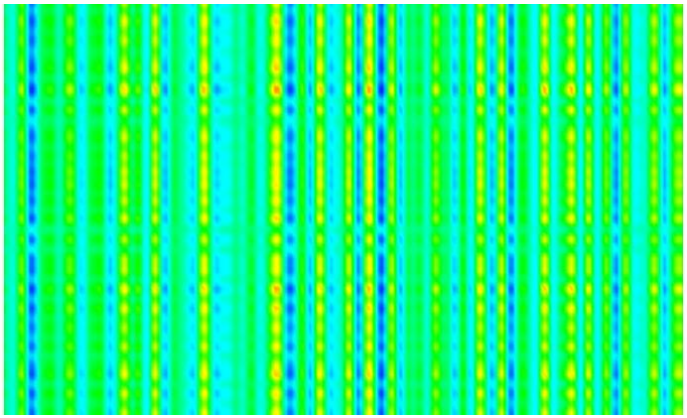

τ = 0.61

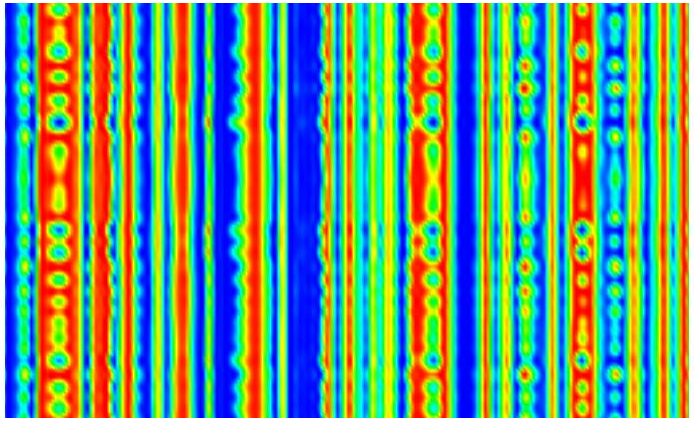

τ = 1.06

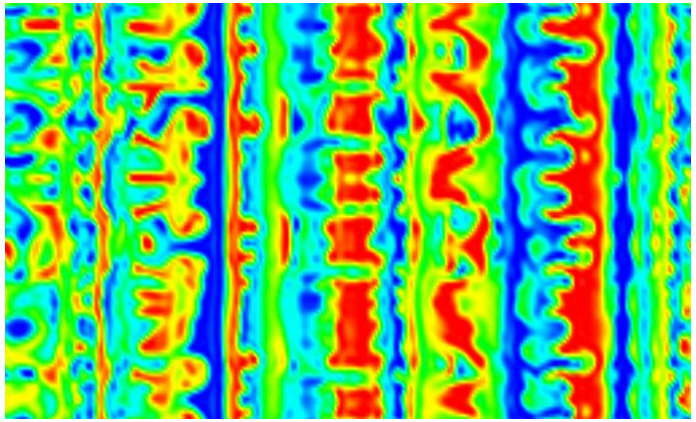

τ = 1.52

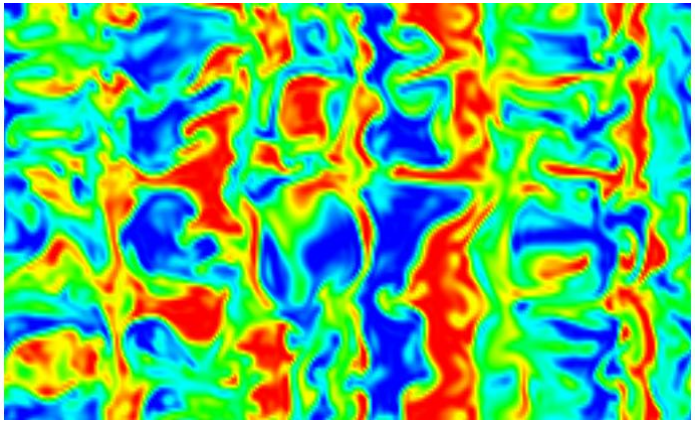

The DNS agrees well with experimental measurements of the bubble/spike front growth and molecular mixing parameter

- DNS and experiment both have a mixing layer growth parameter $\alpha_b \sim 0.07$
- θ on layer centerplane qualitatively agrees with experiment, but under-predicts amount of mixed fluid [$B_0 = \overline{\rho^*}\left(1-\overline{\rho^*}\right) - \overline{\rho^*\left(1-\rho^*\right)}$ and $B_2 = \overline{\rho^*}\left(1-\overline{\rho^*}\right)$ where $\rho^* = (\rho-\rho_2)/(\rho_1-\rho_2) = f_1$]

Bubble, spike fronts

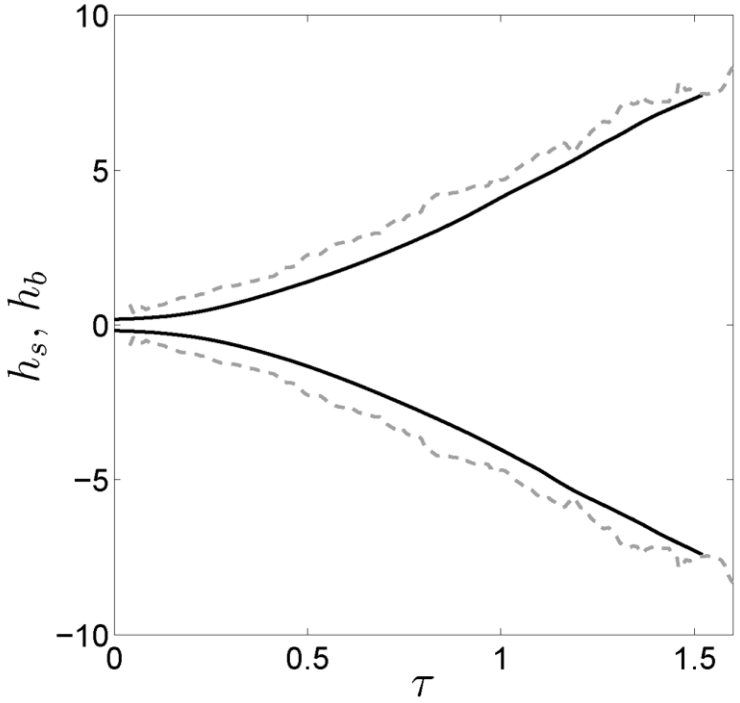

Molecular mixing parameter

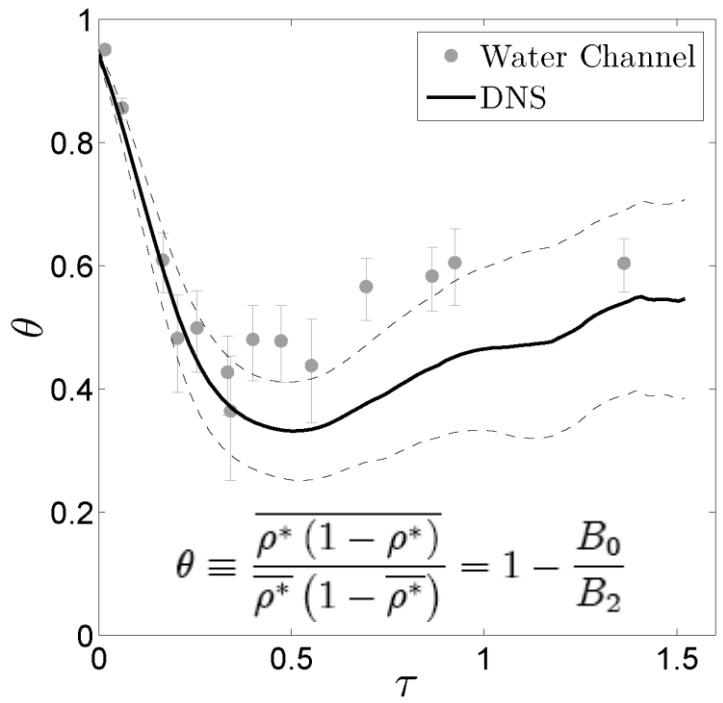

Using averaging over the periodic directions, the exact and closed terms in the transport equations were constructed and compared

- **Unclosed transport equations for turbulent kinetic energy and its dissipation rate, and mass fraction variance and its dissipation rate examined**
- **Production by buoyancy, shear, turbulent fluctuations, and mean field curvature given by P_b^ϕ, P_s^ϕ, P_t^ϕ, and P_c^ϕ, respectively**
- **Conservative transport given by turbulent diffusion T^ϕ and turbulent destruction/dissipation given by D^ϕ**

$$\bar{\rho}\frac{\mathrm{D}\widetilde{E''}}{\mathrm{D}t} = P_b^{\widetilde{E''}} + P_s^{\widetilde{E''}} + \Pi^{\widetilde{E''}} + T^{\widetilde{E''}} - D^{\widetilde{E''}}$$

$$\bar{\rho}\frac{\mathrm{D}\overline{\epsilon'}}{\mathrm{D}t} = P_b^{\overline{\epsilon'}} + P_s^{\overline{\epsilon'}} + P_t^{\overline{\epsilon'}} + P_c^{\overline{\epsilon'}} + T^{\overline{\epsilon'}} - D^{\overline{\epsilon'}}$$

$$\bar{\rho}\frac{\mathrm{D}\widetilde{m_1''^2}}{\mathrm{D}t} = P^{\widetilde{m_1''^2}} + T^{\widetilde{m_1''^2}} - D^{\widetilde{m_1''^2}}$$

$$\bar{\rho}\frac{\mathrm{D}\widetilde{\chi''}}{\mathrm{D}t} = P_s^{\widetilde{\chi''}} + P_b^{\widetilde{\chi''}} + P_t^{\widetilde{\chi''}} + P_c^{\widetilde{\chi''}} + T^{\widetilde{\chi''}} - D^{\widetilde{\chi''}}$$

$$\frac{D}{Dt} = \frac{\partial}{\partial t} + \tilde{u}_j\frac{\partial}{\partial x_j}$$

$$\overline{\phi}(z,t) = \frac{1}{L_x L_y}\int_0^{L_y}\int_0^{L_x}\phi(\mathbf{x},t)\mathrm{d}x\mathrm{d}y$$

$$\widetilde{\phi}(z,t) = \overline{\rho\,\phi(\mathbf{x},t)}/\overline{\rho}$$

$$\phi(\mathbf{x},t)' = \phi(\mathbf{x},t) - \overline{\phi}(z,t)$$

$$\phi(\mathbf{x},t)'' = \phi(\mathbf{x},t) - \widetilde{\phi}(z,t)$$

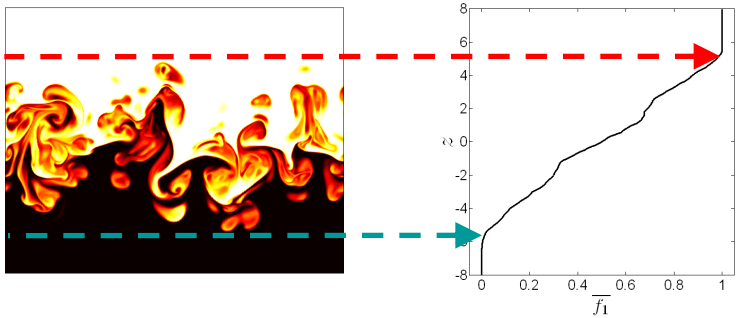

The turbulent viscosity is computed using the turbulent kinetic energy and its dissipation rate

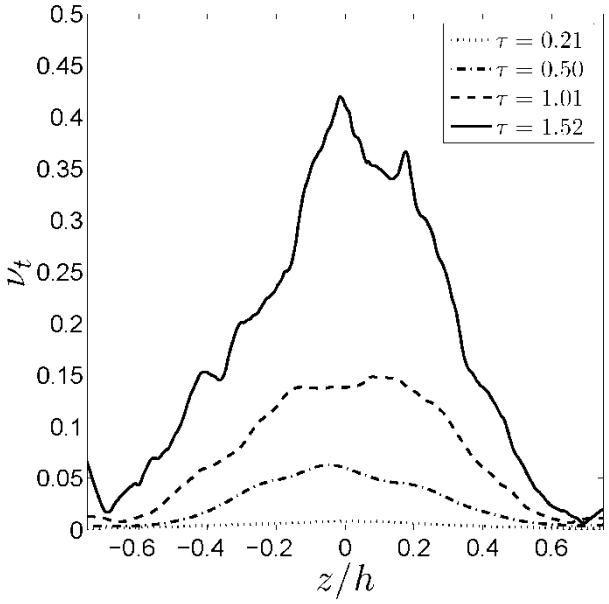

All vertical profiles across mixing layer rescaled by mixing layer width *h*(*t*)

- **Turbulent viscosity computed using shear turbulence value C_μ = 0.09**

$$\nu_t = C_\mu \frac{\left(\widetilde{E''}\right)^2}{\widetilde{\epsilon''}}$$

- **Profiles peaked near center of layer where turbulence most intense**
- **Asymmetry may be associated with anisotropic initial conditions**
- **$\nu_t > \nu = 0.1$ as turbulence develops**

DNS data can be used to compute each unclosed term in the turbulent kinetic energy equation

Buoyancy production

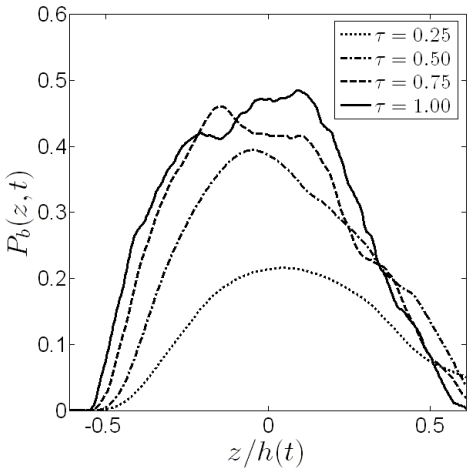

Shear

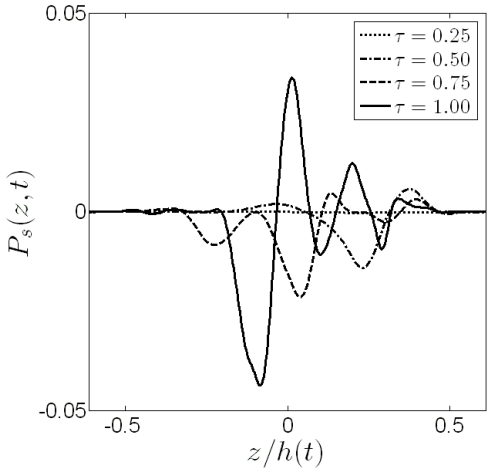

Turbulent diffusion

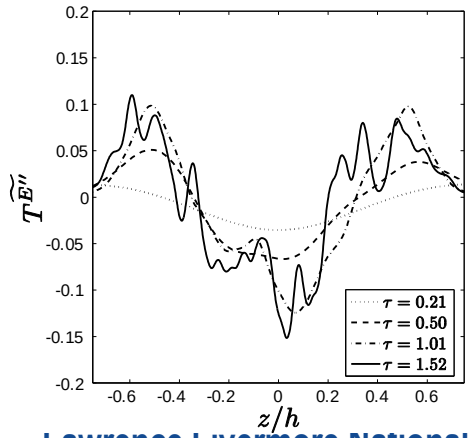

Dissipation

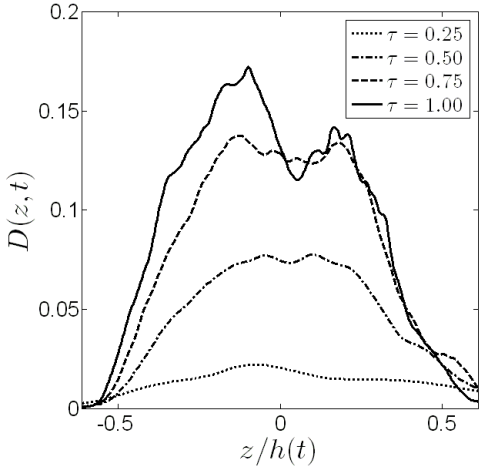

- **Buoyancy production and dissipation approximately parabolic, consistent with similarity solutions**
- **Shear term small and oscillates, consistent with nearly zero mean velocity gradient**
- **Diffusion has complex structure, integrating to zero across domain, as required**

DNS data can be used to compute each unclosed term in the turbulent kinetic energy dissipation rate equation

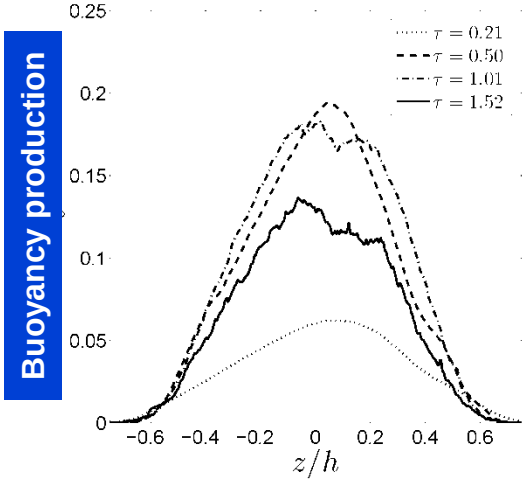

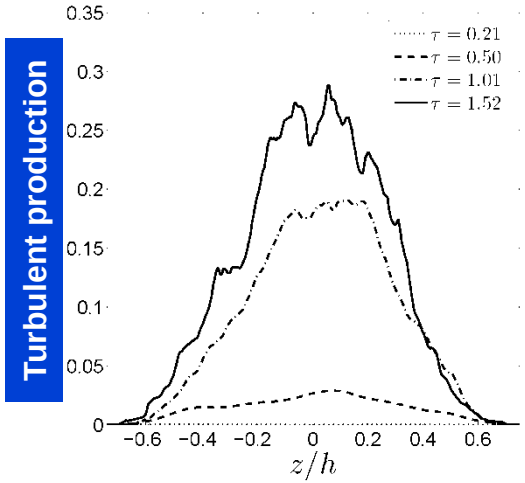

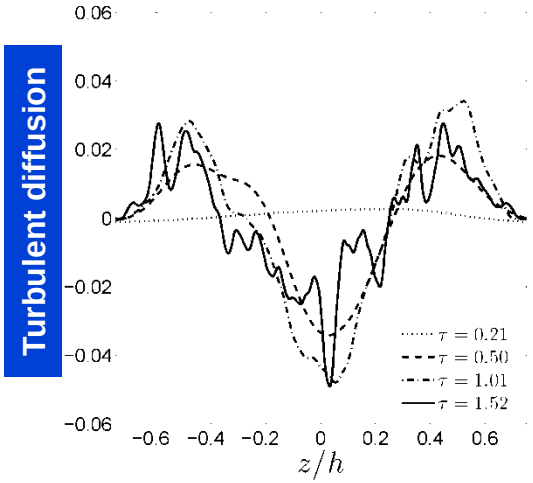

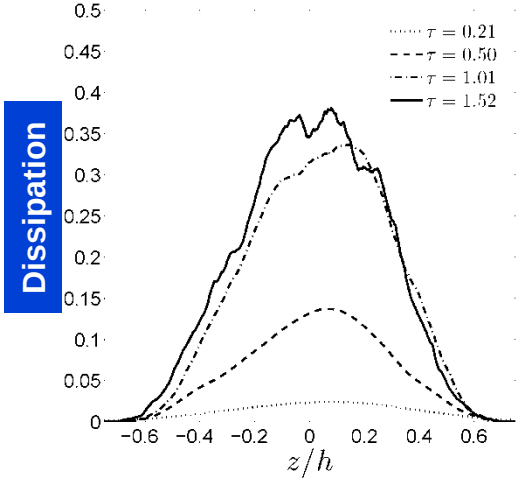

$$P_b^{\overline{\epsilon'}} = 2\,\nu\, g_i \overline{\frac{\partial u_i'}{\partial x_j}\frac{\partial p'}{\partial x_j}}$$

$$P_t^{\overline{\epsilon'}} = -2\,\mu \overline{\frac{\partial u_i'}{\partial x_k}\frac{\partial u_i'}{\partial x_m}\frac{\partial u_k'}{\partial x_m}}$$

$$T^{\overline{\epsilon'}} = \frac{\partial}{\partial x_j}\left(\mu\frac{\partial \overline{\epsilon'}}{\partial x_j} - \overline{\epsilon'\,u_j'} - 2\,\nu \overline{\frac{\partial p'}{\partial x_m}\frac{\partial u_j'}{\partial x_m}}\right)$$

$$D^{\overline{\epsilon'}} = 2\,\nu^2\,\overline{\rho}\overline{\left(\frac{\partial^2 u_i'}{\partial x_k \partial x_k}\right)^2}$$

- **Turbulent production dominates buoyancy production for $\tau > 1$**
- **Transport away from turbulent core, down-gradient**
- **Mean velocity production terms negligible**

$\tau = 0.21$	$Re_h = 67$
$\tau = 0.50$	$Re_h = 481$
$\tau = 1.01$	$Re_h = 2323$
$\tau = 1.52$	$Re_h = 4455$

The budget of the unclosed mass fraction variance transport equation can also be computed using DNS data

Mean production

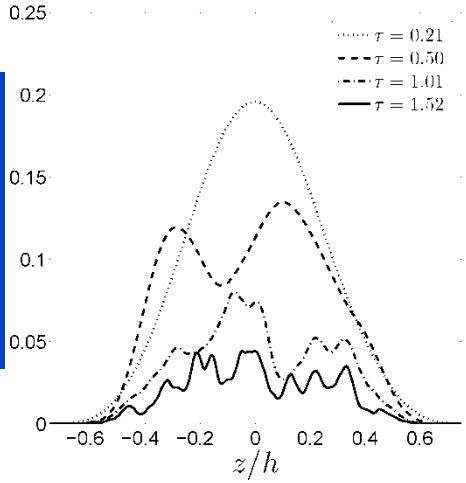

Dissipation

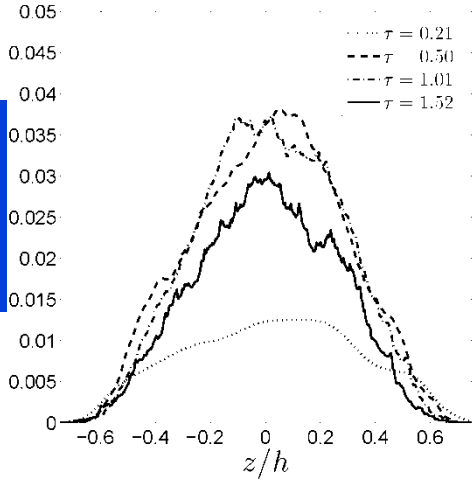

$$P^{\widetilde{m_1''^2}} = -2\,\overline{\rho\, u_j''\, m_1''}\,\frac{\partial \widetilde{m}_1}{\partial x_j}$$

$$T^{\widetilde{m_1''^2}} = \frac{\partial}{\partial x_j}\left(\overline{\rho\, D\,\frac{\partial m_1''^2}{\partial x_j}} - \overline{\rho\, u_j''\, m_1''^2}\right)$$

$$D^{\widetilde{m_1''^2}} = 2\,\overline{\rho}\,\widetilde{\chi''} = 2\,\overline{\rho\, D\left(\frac{\partial m_1''}{\partial x_j}\right)^2}$$

Turbulent diffusion

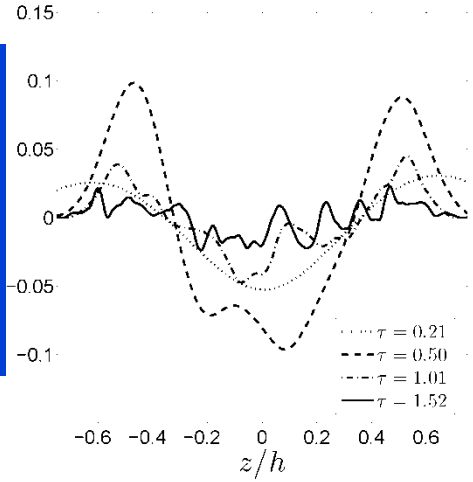

$\tau = 0.21$	$Re_h = 67$
$\tau = 0.50$	$Re_h = 481$
$\tau = 1.01$	$Re_h = 2323$
$\tau = 1.52$	$Re_h = 4455$

- Buoyancy production decreases in time as mixing progresses
- Production ≈ dissipation at late time
- Transport away from turbulent core, down-gradient

Some terms in the mass fraction variance dissipation rate equation behave similarly to those in the $\overline{\epsilon'}$ equation, while others do not

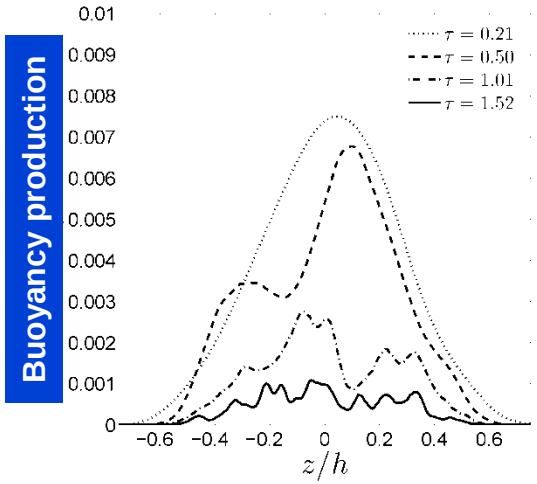

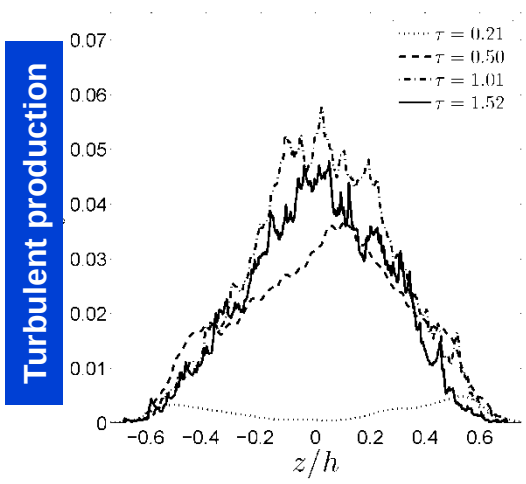

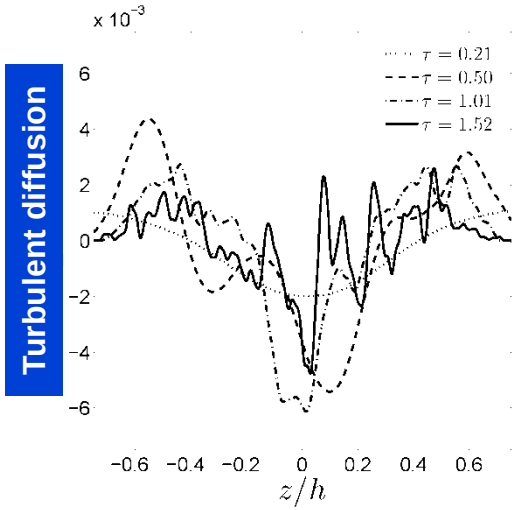

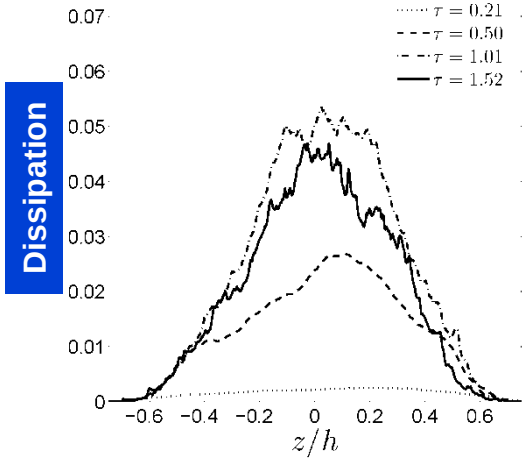

$$P_b^{\widetilde{\chi''}} = -2\,\rho\,D\,\overline{\frac{\partial m_1''}{\partial x_i}\frac{\partial u_j''}{\partial x_i}\frac{\partial \tilde{m}_1}{\partial x_j}}$$

$$P_t^{\widetilde{\chi''}} = 2\,\rho\,D\,\overline{\frac{\partial m_1''}{\partial x_i}\frac{\partial m_1''}{\partial x_j}\frac{\partial u_j''}{\partial x_i}}$$

$$T^{\widetilde{\chi''}} = -\frac{\partial}{\partial x_j}\left(\overline{\rho}\,D\,\frac{\partial \widetilde{\chi''}}{\partial x_j} - \overline{\rho}\,\widetilde{\chi''\,u_j''}\right)$$

$$D^{\widetilde{\chi''}} = 2\,D^2\,\overline{\rho\left(\frac{\partial^2 m_1''}{\partial x_i \partial x_j}\right)^2}$$

- **Mass fraction dissipation rate controls mixing rate**
- **Buoyancy production small and decreases in time**
- **As in $\overline{\epsilon'}$ transport, turbulent production dominates at late time**

$\tau = 0.21$	$Re_h = 67$
$\tau = 0.50$	$Re_h = 481$
$\tau = 1.01$	$Re_h = 2323$
$\tau = 1.52$	$Re_h = 4455$

The previous equations are closed using gradient-diffusion and similarity closures

- **Gradient-diffusion closures**

$$\widetilde{\phi'' u_j''} = -\frac{\nu_t}{\sigma_\phi}\frac{\partial \widetilde{\phi}}{\partial x_j} \qquad \nu_t = \frac{\mu_t}{\overline{\rho}} = C_\mu \frac{\left(\widetilde{E''}\right)^2}{\overline{\epsilon'}}$$

- **Similarity closures in $\overline{\epsilon'}$ and $\widetilde{m_1''^2}$ equations ($C_{\varepsilon 0}$, $C_{\varepsilon 2}$, C_{m2} are model coefficients)**

$$P_b^{\overline{\epsilon'}} = 2\,\overline{\nu}\,g_i\,\overline{\frac{\partial \rho'}{\partial x_j}\frac{\partial u_i'}{\partial x_j}} = C_{\epsilon 0}\frac{\overline{\epsilon'}}{\widetilde{E''}}\frac{\nu_t}{\sigma_\rho\,\overline{\rho}}\frac{\partial \overline{\rho}}{\partial x_j}\frac{\partial \overline{p}}{\partial x_j}$$

$$D^{\overline{\epsilon'}} - P_t^{\overline{\epsilon'}} = 2\,\overline{\mu}\,\overline{\nu}\,\overline{\left(\frac{\partial^2 u_i'}{\partial x_j \partial x_k}\right)^2} + 2\,\overline{\mu}\,\overline{\frac{\partial u_i'}{\partial x_j}\frac{\partial u_i'}{\partial x_k}\frac{\partial u_j'}{\partial x_k}} = C_{\epsilon 2}\,\overline{\rho}\,\frac{\left(\overline{\epsilon'}\right)^2}{\widetilde{E''}}$$

$$D^{\widetilde{m_1''^2}} = 2\,\rho\,D\,\overline{\left(\frac{\partial m_1''}{\partial x_j}\right)^2} = 2\,C_{m2}\,\overline{\rho}\,\frac{\overline{\epsilon'}}{\widetilde{E''}}\,\widetilde{m_1''^2}$$

Gradient-diffusion closures for all equations and similarity closures for mass fraction variance dissipation rate equations

$$\overline{\rho' u_j'} = -\frac{\nu_t}{\sigma_\rho}\frac{\partial \overline{\rho}}{\partial x_j} \qquad \widetilde{m_1'' u_j'} = -\frac{\nu_t}{\sigma_m}\frac{\partial \widetilde{m}_1}{\partial x_j}$$

$$\widetilde{E'' u_j'} = -\frac{\nu_t}{\sigma_k}\frac{\partial \widetilde{E''}}{\partial x_j} \qquad \overline{\epsilon' u_j'} = -\frac{\nu_t}{\sigma_\epsilon}\frac{\partial \overline{\epsilon'}}{\partial x_j}$$

$$\widetilde{m_1''^2 u_j'} = -\frac{\nu_t}{\sigma_{m2}}\frac{\partial \widetilde{m_1''^2}}{\partial x_j} \qquad \widetilde{\chi'' u_j'} = -\frac{\nu_t}{\sigma_\chi}\frac{\partial \widetilde{\chi''}}{\partial x_j}$$

$$P_m^{\widetilde{\chi''}} = -2\,\rho\,D\,\overline{\frac{\partial m_1''}{\partial x_i}\frac{\partial u_j''}{\partial x_i}\frac{\partial \widetilde{m}_1}{\partial x_j}} = C_{\chi 0}\,\mu_t\,\frac{\overline{\epsilon'}}{\widetilde{E''}}\left(\frac{\partial \widetilde{m}_1}{\partial x_j}\right)^2$$

$$P_t^{\widetilde{\chi''}} = 2\,\rho\,D\,\overline{\frac{\partial m_1''}{\partial x_i}\frac{\partial m_1''}{\partial x_j}\frac{\partial u_j''}{\partial x_i}} = C_{\chi 2}\,\overline{\rho}\,\frac{\overline{\epsilon'}}{\widetilde{E''}}\,\widetilde{m_1''^2}$$

$$D^{\widetilde{\chi''}} = 2\,\rho\,D^2\,\overline{\left(\frac{\partial^2 m_1''}{\partial x_i \partial x_j}\right)^2} = C_{\chi 3}\,\overline{\rho}\,\frac{\left(\widetilde{\chi''}\right)^2}{\widetilde{m_1''^2}}$$

Gradient-diffusion closures using dynamic coefficients agree well with the exact turbulent fluxes (τ = 1.01)

$$\widetilde{\phi'' u_j''} = -\frac{\nu_t}{\sigma_\phi}\frac{\partial \widetilde{\phi}}{\partial x_j}$$

- **Gradient-diffusion models for turbulent diffusion terms appropriate**
- **Oscillations in model due to gradient of mean field quantities**

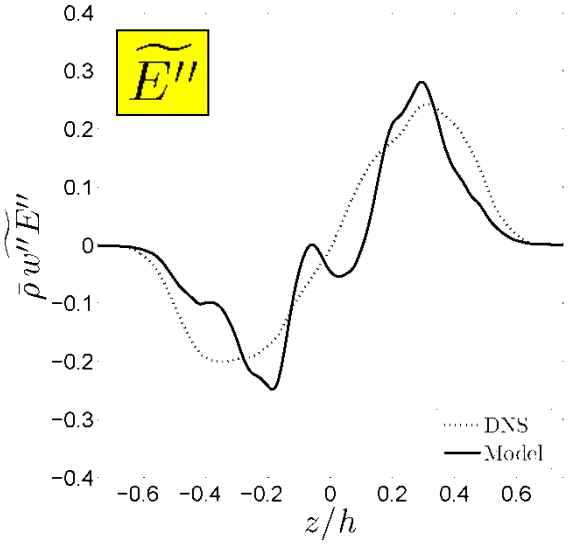

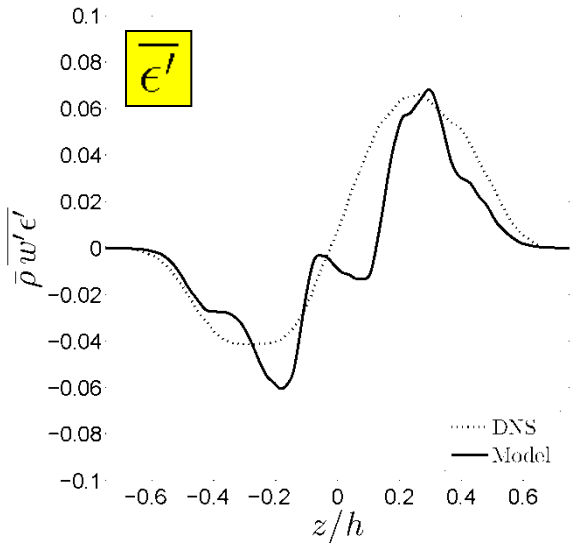

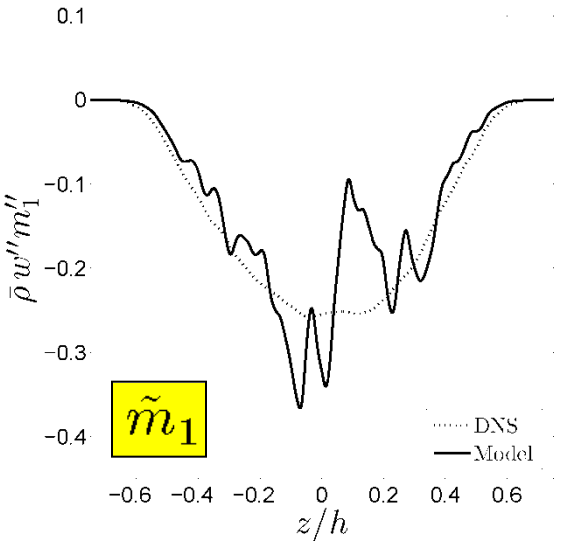

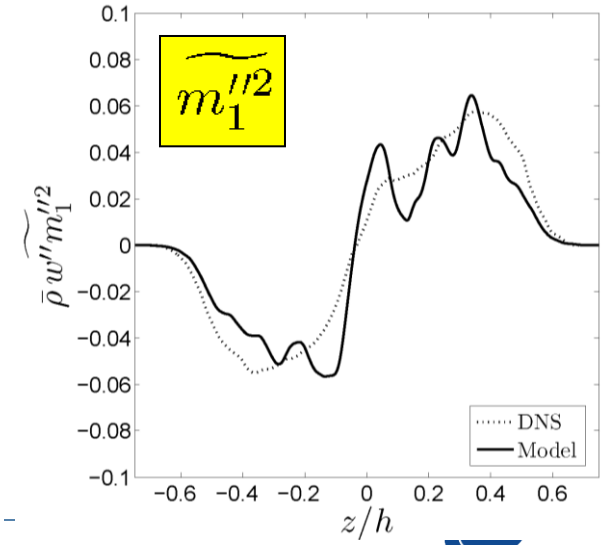

The turbulent Schmidt numbers were calibrated by correlating the closures with the exact terms computed from the DNS data

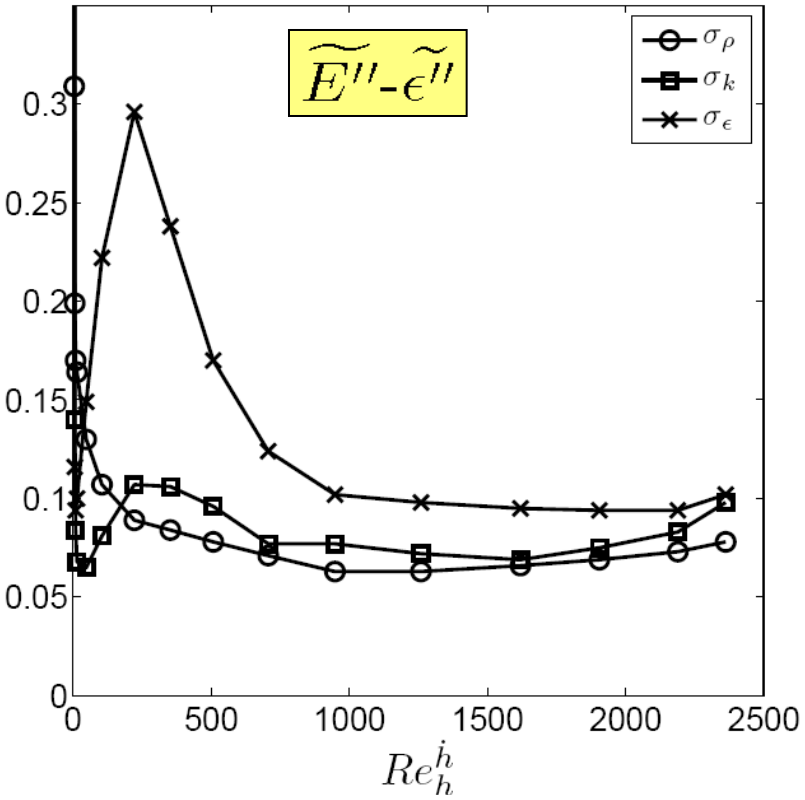

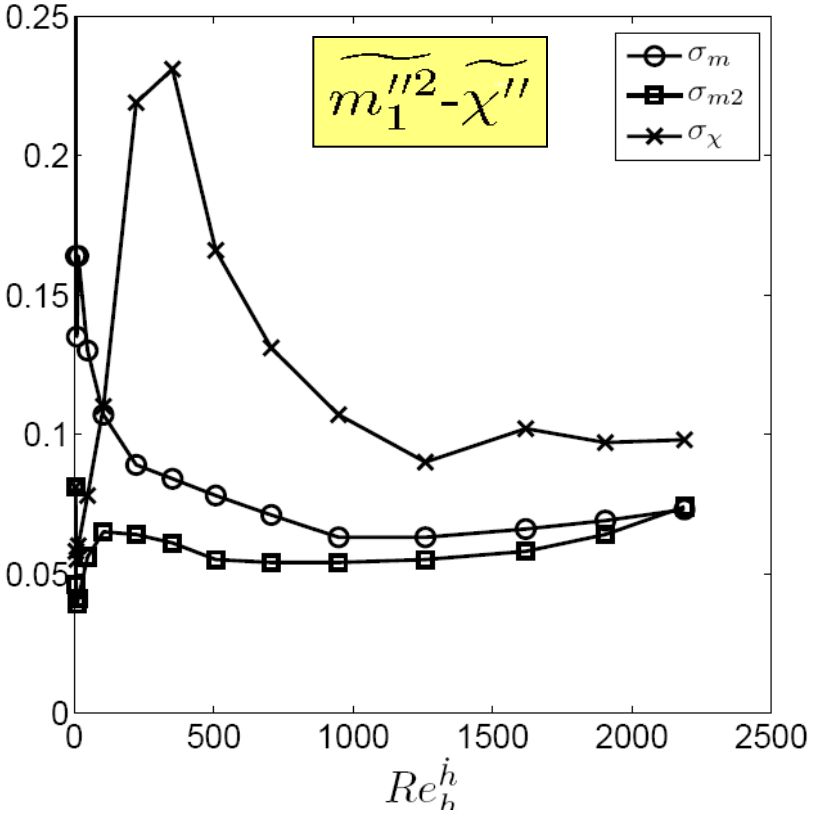

- **Turbulent Schmidt numbers (except σ_ε) nearly constant for τ > 0.75**
- **Late-time rise in σ_ε, σ_{m2} and σ_χ may be due to oscillations in DNS data**
- **Self-similarity requires $\sigma_\rho = \sigma_k = \sigma_m$ (≈ 0.1) consistent with data**

Similarly, similarity closures using dynamic coefficients agree well with the exact production and dissipation terms ($\tau = 1.01$)

- **Similarity closures for more complex correlations are in very good agreement with DNS**

$$P_b^{\overline{\epsilon'}} = C_{\epsilon 0}\,\frac{\overline{\epsilon'}}{\widetilde{E''}}\,P_b^{\widetilde{E''}} \qquad D^{\overline{\epsilon'}} - P_t^{\overline{\epsilon'}} = C_{\epsilon 2}\,\bar{\rho}\,\frac{\left(\overline{\epsilon'}\right)^2}{\widetilde{E''}} \qquad \widetilde{\chi''} = C_{m2}\,\frac{\overline{\epsilon'}}{\widetilde{E''}}\,\widetilde{m_1''^2}$$

Buoyancy Production

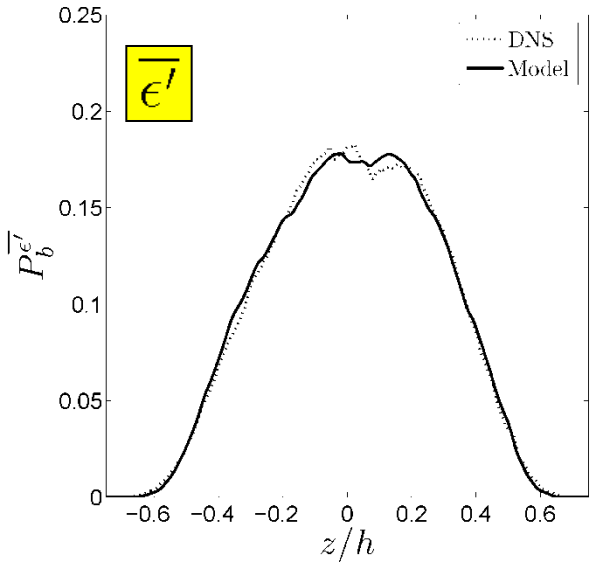

Turbulent Destruction

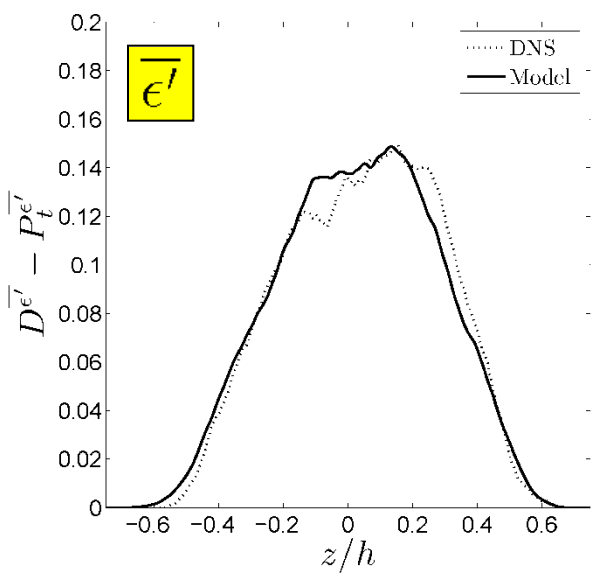

Turbulent Destruction

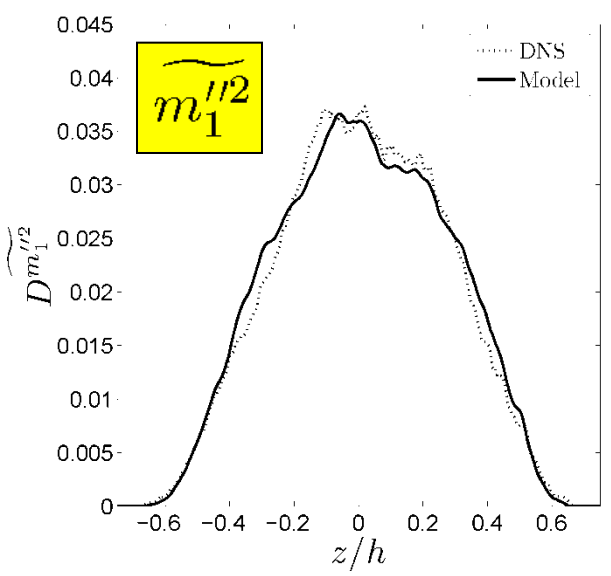

Similarity coefficients in the dissipation rate equations were also calibrated as a function of the Reynolds number

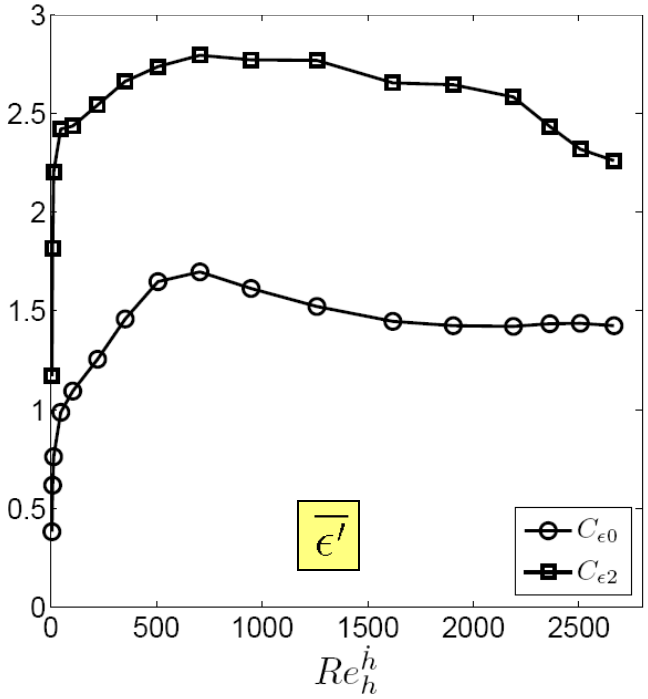

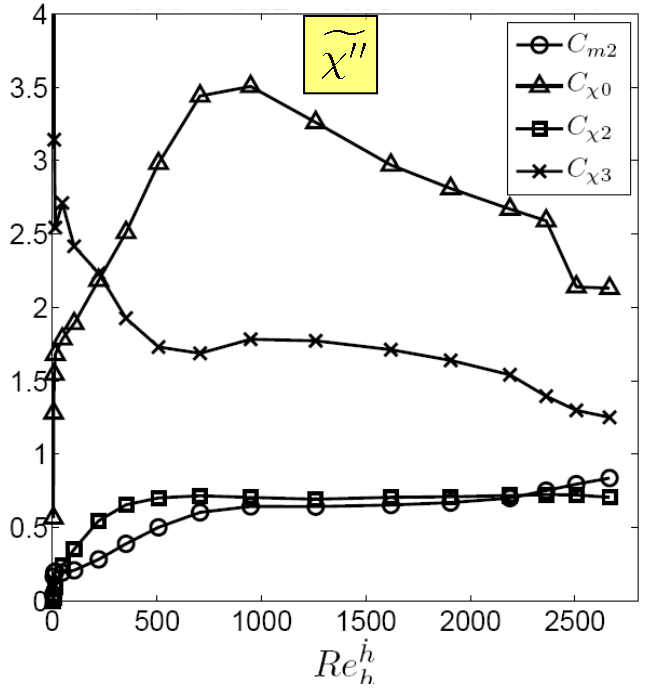

- $C_{\varepsilon 0} \approx 1.4$; $C_{\varepsilon 2} \approx 2.3$ (decreasing at late times)
- C_{m2} and $C_{\chi 3}$ still evolving at late times, as fully asymptotic mixing not attained; $C_{\chi 0}$ and $C_{\chi 2}$ approximately constant
- Using late-time coefficient values, self-similarity gives

$$\alpha_b = \frac{C_\mu}{\sigma_\rho} \frac{\left(C_{\epsilon 2} - C_{\epsilon 0}\right)^2}{\left(4\,C_{\epsilon 0} - 3\right)\left(4\,C_{\epsilon 2} - 3\right)} \approx 0.05$$

The optimized RANS model was tested *a posteriori* using a one-dimensional numerical implementation of the model

- **Modeled transport equations solved using 2nd-order finite differencing and a 2nd-order Crank–Nicolson time integration**

$$\bar{\rho}\,\frac{\partial \tilde{m}_1}{\partial t} = \frac{\partial}{\partial z}\left[\left(\frac{\bar{\mu}}{Sc} + \frac{\mu_t}{\sigma_m}\right)\frac{\partial \tilde{m}_1}{\partial z}\right]$$

$$\bar{\rho}\,\frac{\partial \widetilde{E''}}{\partial t} = -\frac{\nu_t}{\sigma_\rho\,\bar{\rho}}\,\frac{\partial \bar{\rho}}{\partial z}\,\frac{\partial \bar{p}}{\partial z} + \frac{\partial}{\partial z}\left[\left(\bar{\mu} + \frac{\mu_t}{\sigma_k}\right)\frac{\partial \widetilde{E''}}{\partial z}\right] - \bar{\rho}\,\widetilde{\epsilon''}$$

$$\bar{\rho}\,\frac{\partial \widetilde{\epsilon''}}{\partial t} = -C_{\epsilon_0}\,\frac{\widetilde{\epsilon''}}{\widetilde{E''}}\,\frac{\nu_t}{\sigma_\rho\,\bar{\rho}}\,\frac{\partial \bar{\rho}}{\partial z}\,\frac{\partial \bar{p}}{\partial z} + \frac{\partial}{\partial z}\left[\left(\bar{\mu} + \frac{\mu_t}{\sigma_\epsilon}\right)\frac{\partial \widetilde{\epsilon''}}{\partial z}\right] - C_{\epsilon 2}\,\bar{\rho}\,\frac{\left(\widetilde{\epsilon''}\right)^2}{\widetilde{E''}}$$

$$\bar{\rho}\,\frac{\partial \widetilde{m_1''^2}}{\partial t} = 2\,\frac{\mu_t}{\sigma_m}\left(\frac{\partial \tilde{m}_1}{\partial z}\right)^2 + \frac{\partial}{\partial z}\left[\left(\frac{\bar{\mu}}{Sc} + \frac{\mu_t}{\sigma_{m2}}\right)\frac{\partial \widetilde{m_1''^2}}{\partial z}\right] - 2\,\bar{\rho}\,\widetilde{\chi''}$$

$$\bar{\rho}\,\frac{\partial \widetilde{\chi''}}{\partial t} = C_{\chi 0}\,\mu_t\,\frac{\widetilde{\epsilon''}}{\widetilde{E''}}\left(\frac{\partial \tilde{m}_1}{\partial z}\right)^2 + \frac{\partial}{\partial z}\left[\left(\frac{\bar{\mu}}{Sc} + \frac{\mu_t}{\sigma_\chi}\right)\frac{\partial \widetilde{\chi''}}{\partial z}\right] + \bar{\rho}\,\widetilde{\chi''}\left(C_{\chi 2}\frac{\widetilde{\epsilon''}}{\widetilde{E''}} - C_{\chi 3}\frac{\widetilde{\chi''}}{\widetilde{m_1''^2}}\right)$$

The model was run using both dynamic and constant (late-time) coefficients

The growth of the mixing layer and the evolution of the molecular mixing parameter compare favorably with the DNS

- **Model initialized using DNS data at times τ_{IC} = 0.1, 0.3, 0.5, 0.7 to test early-time model dynamics**
- **Model with τ_{IC} = 0.1 cannot capture complex early-time physics**
- **For τ > 0.8, all model instantiations give very similar layer growth and θ**

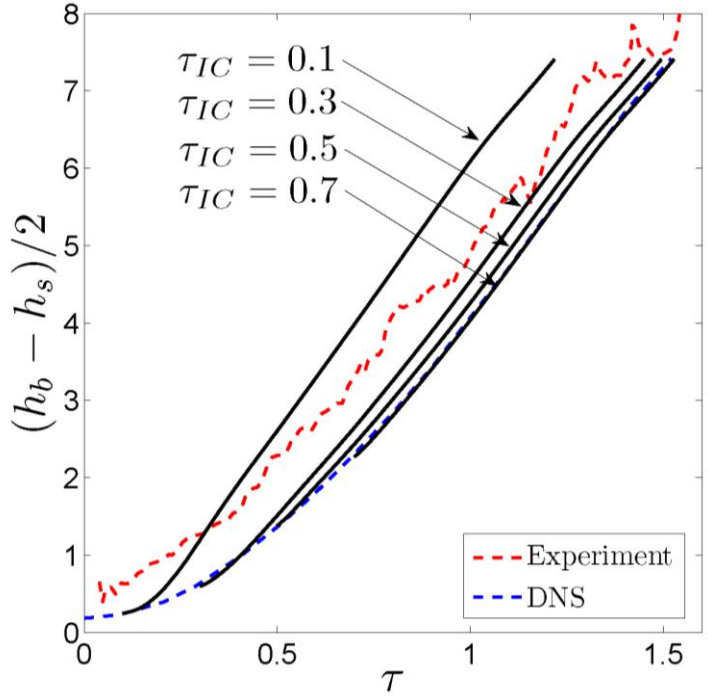

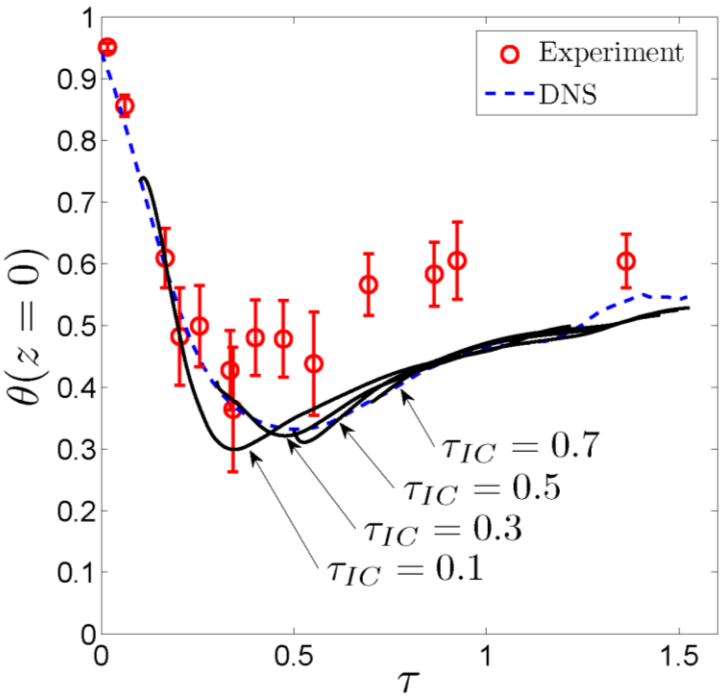

The production-to-dissipation ratios from the DNS and model with dynamic and constant coefficients can be compared

- ***Re*-dependent coefficients capture early-time transitional dynamics**
- **Constant coefficient case fails to capture nonequilibrium behavior**

Dynamic coefficient case

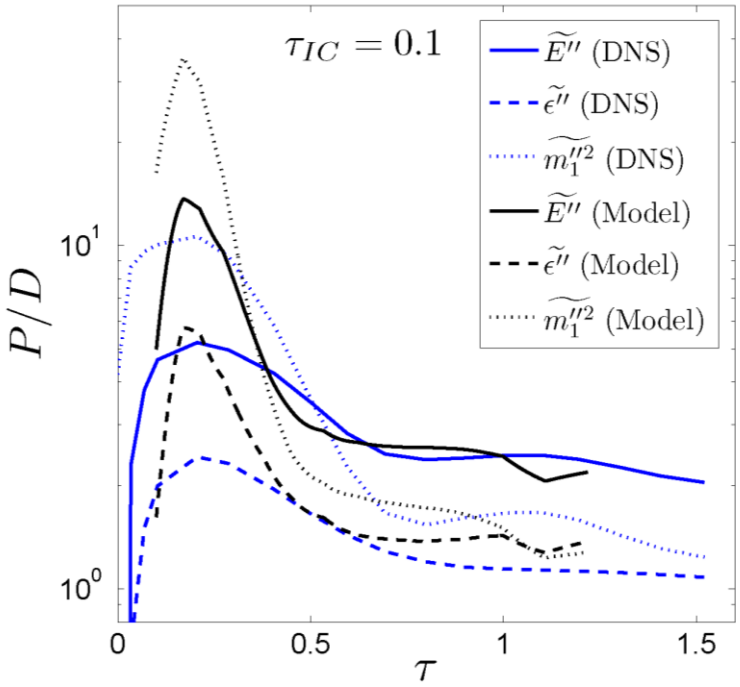

Constant coefficient case

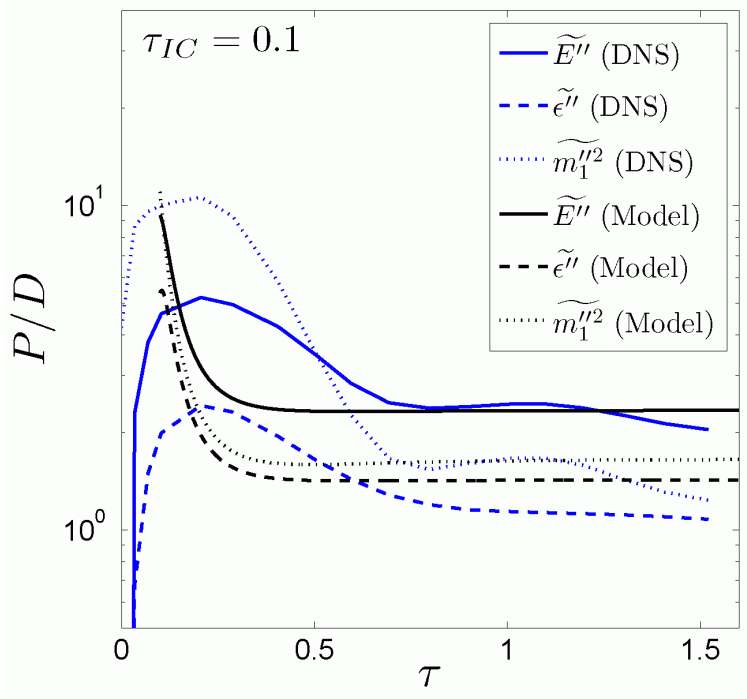

The model predicts a θ in good agreement with the experimental measurement using the recalibrated C_{m2}

- Growth of $Pr = 7$ and $Sc \sim 10^3$ mixing layers similar, which allows use of DNS profiles of $\widetilde{P^{m_1''^2}}$, $\widetilde{E''}$, and $\overline{\epsilon'}$ to first-order
- Mass fraction variance profiles taken from $Sc \sim 10^3$ experiments
- Calibrated C_{m2} for $Sc \sim 10^3$ smaller than C_{m2} for $Sc = 7$

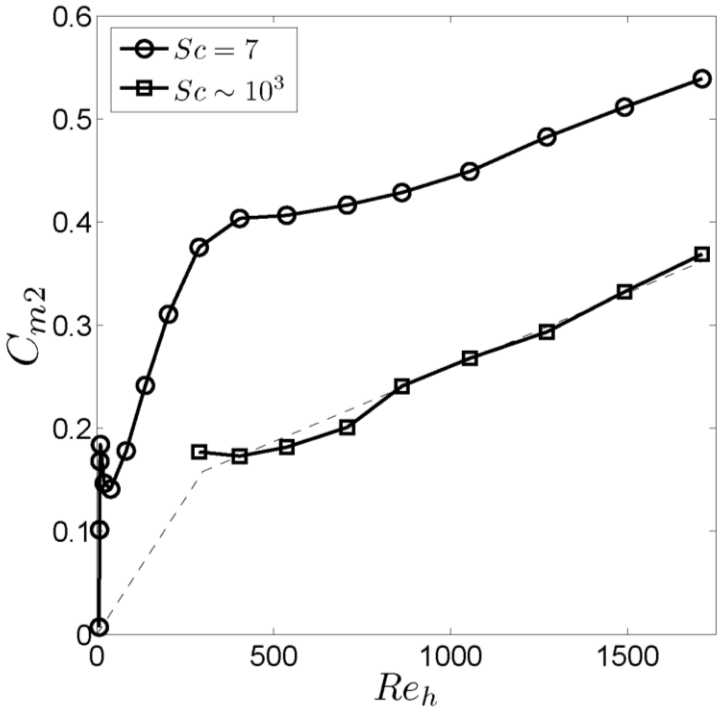

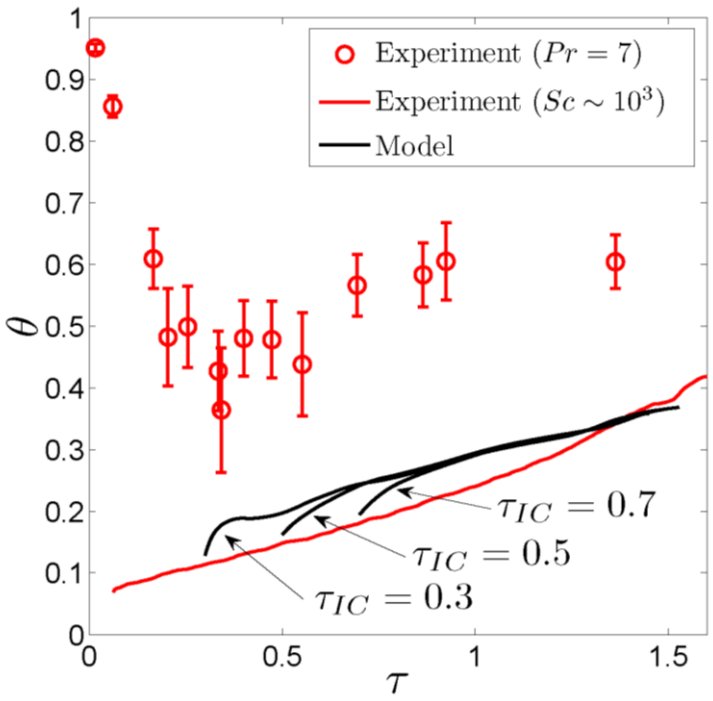

A 3- or 4-equation turbulence model for Rayleigh–Taylor mixing was developed using optimized coefficients from DNS data

- **Examined gradient-diffusion/similarity closures**
  - **Used data to compute exact unclosed terms in transport equations**
  - ***A priori* analysis and optimization using DNS data**
  - **Buoyancy/turbulent production, dissipation, and diffusion are dominant physical processes requiring accurate modeling**
- **Correlating models and terms computed from data gives *Re*-dependent coefficients**
- **Some coefficients asymptote and others continue to evolve at late times**
  - **Demonstrated very good agreement between models and DNS data using these Reynolds number-dependent coefficients**

A DNS model of a water channel experiment was used to develop an *a priori calibrated RANS model for Sc = 7 Rayleigh–Taylor mixing*, and data from the DNS and experiment were combined to provide a *RANS model for a Sc ~ 10^3 Rayleigh–Taylor mixing layer*

A very high Reynolds number 3072^3 DNS dataset[3] was used to analyze gradient-diffusion and similarity closures for Rayleigh–Taylor mixing[4]

- 3:1 density ratio (Atwood number 0.5)
- Schmidt number $\nu / D = 1$
- $Re = (h\, dh/dt) / \nu > 10^4$ achieved at late times $18 < t/t_0 < 30$
- Grid spacing equal to Kolmogorov scale at $t/t_0 = 30$
- Diffuse initial interface with Gaussian perturbations around $k = 96$

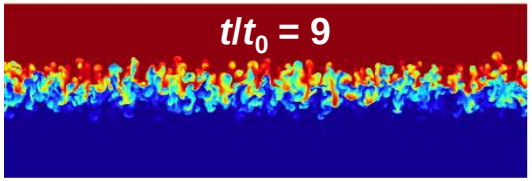

$Re \sim 2 \times 10^3$

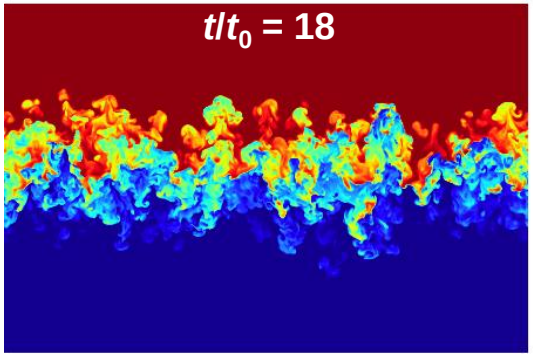

$Re \sim 8 \times 10^3$

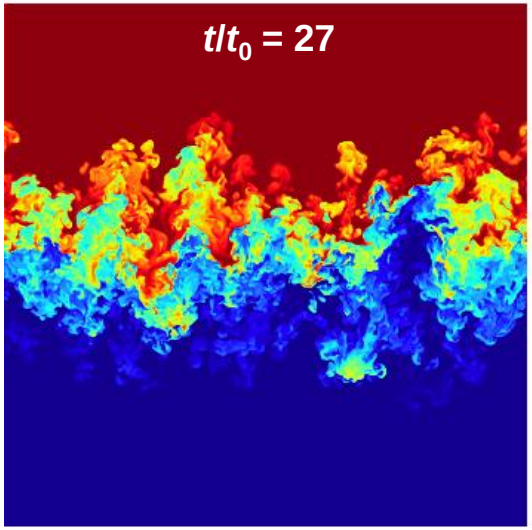

$Re \sim 2.2 \times 10^4$

[3]W. H. Cabot & A. W. Cook, "Reynolds number effects on Rayleigh–Taylor instability with possible implications for type-Ia supernovae," *Nat. Phys*. 2, 562 (2006)

[4]O. Schilling & G. C. Burton, "Large-Reynolds-number, intermediate-Atwood-number Rayleigh–Taylor turbulence: Gradient-diffusion and similarity modeling of mechanical and scalar turbulence," (submitted)

The dominant terms in the mechanical and scalar turbulent transport equations can be identified using the DNS data (shown here at $t/t_0 = 27$)

Turbulent Kinetic Energy Budget

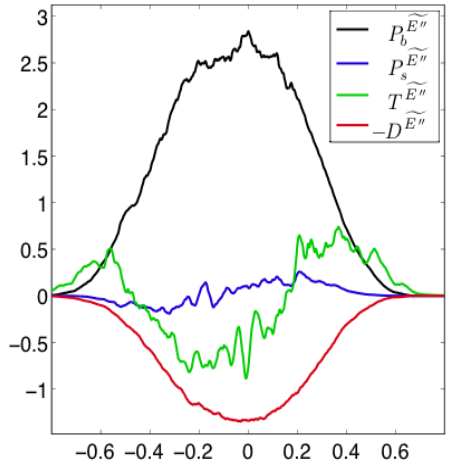

Turbulent Dissipation Budget

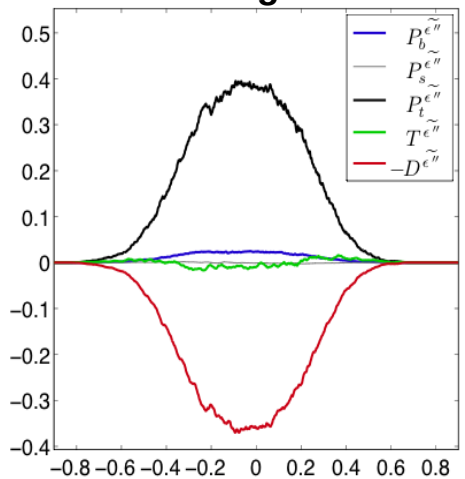

$$\overline{\rho}\,\frac{\partial \widetilde{E''}}{\partial t} \approx P_b^{\widetilde{E''}} + P_s^{\widetilde{E''}} - D^{\widetilde{E''}} + T^{\widetilde{E''}}$$

$$\overline{\rho}\,\frac{\partial \widetilde{\epsilon''}}{\partial t} \approx P_b^{\widetilde{\epsilon''}} + P_s^{\widetilde{\epsilon''}} + P_t^{\widetilde{\epsilon''}} - D^{\widetilde{\epsilon''}} + T^{\widetilde{\epsilon''}}$$

Buoyancy production, dissipation, and transport are most important in *K* equation; turbulent production and destruction are most important in ε equation

Density Variance Budget

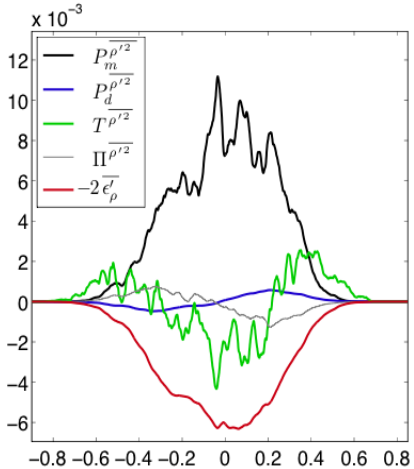

Density Variance Dissipation Budget

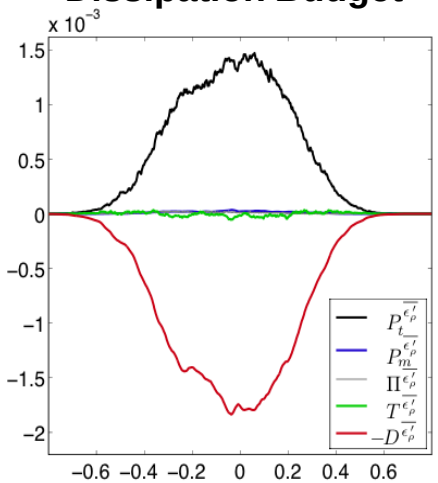

$$\frac{\partial \overline{\rho'^2}}{\partial t} \approx P_m^{\overline{\rho'^2}} + P_d^{\overline{\rho'^2}} - 2\,\overline{\epsilon'_\rho} + \Pi^{\overline{\rho'^2}} + T^{\overline{\rho'^2}}$$

$$\frac{\partial \overline{\epsilon'_\rho}}{\partial t} \approx P_t^{\overline{\epsilon'_\rho}} + P_m^{\overline{\epsilon'_\rho}} - D^{\overline{\epsilon'_\rho}} + \Pi^{\overline{\epsilon'_\rho}} + T^{\overline{\epsilon'_\rho}}$$

Mean production, dissipation, and transport are most important in $\overline{\rho'^2}$ equation; turbulent production and transport are most important in $\overline{\epsilon'_\rho}$ equation

A buoyancy-generalized Boussinesq model for the Reynolds stresses provides quite good agreement with DNS at all times

- **Generalized Boussinesq model**

$$\tau_{ij} = \underbrace{\frac{2}{3}\overline{\rho}\,\widetilde{E''}\,\delta_{ij} - 2\,\mu_t\left(\widetilde{S}_{ij} - \frac{\delta_{ij}}{3}\frac{\partial \widetilde{u}_k}{\partial x_k}\right)}_{\text{Boussinesq}} - C_A^{(ij)}\,\nu_t\,\frac{\widetilde{E''}}{\overline{\rho}\,\widetilde{\epsilon''}}\,\overline{A}_{ij}$$

$$\overline{A}_{ij} \equiv \frac{\partial \overline{\rho}}{\partial x_i}\frac{\partial \overline{p}}{\partial x_j} + \frac{\partial \overline{\rho}}{\partial x_j}\frac{\partial \overline{p}}{\partial x_i} - \frac{2}{3}\delta_{ij}\frac{\partial \overline{\rho}}{\partial x_k}\frac{\partial \overline{p}}{\partial x_k}$$

- **Adapted from algebraic stress model for turbulent convection**

$$\overline{v_i' v_j'} = \frac{2}{3}\overline{E'}\,\delta_{ij} - 2\,\nu_t\,\overline{S}_{ij}$$
$$+C_T\,\beta\,\frac{\overline{E'}}{\overline{\epsilon'}}\left(g_i\,\overline{T' u_j'} + g_j\,\overline{T' u_i'} - \frac{2}{3}\delta_{ij}\,g_k\,\overline{T' u_k'}\right)$$

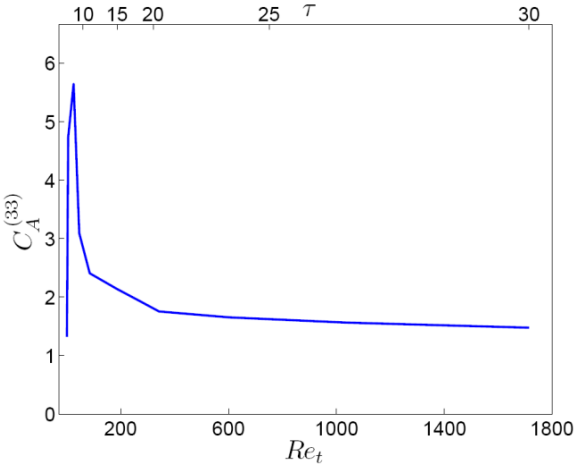

$t/t_0 = 9$ $t/t_0 = 27$

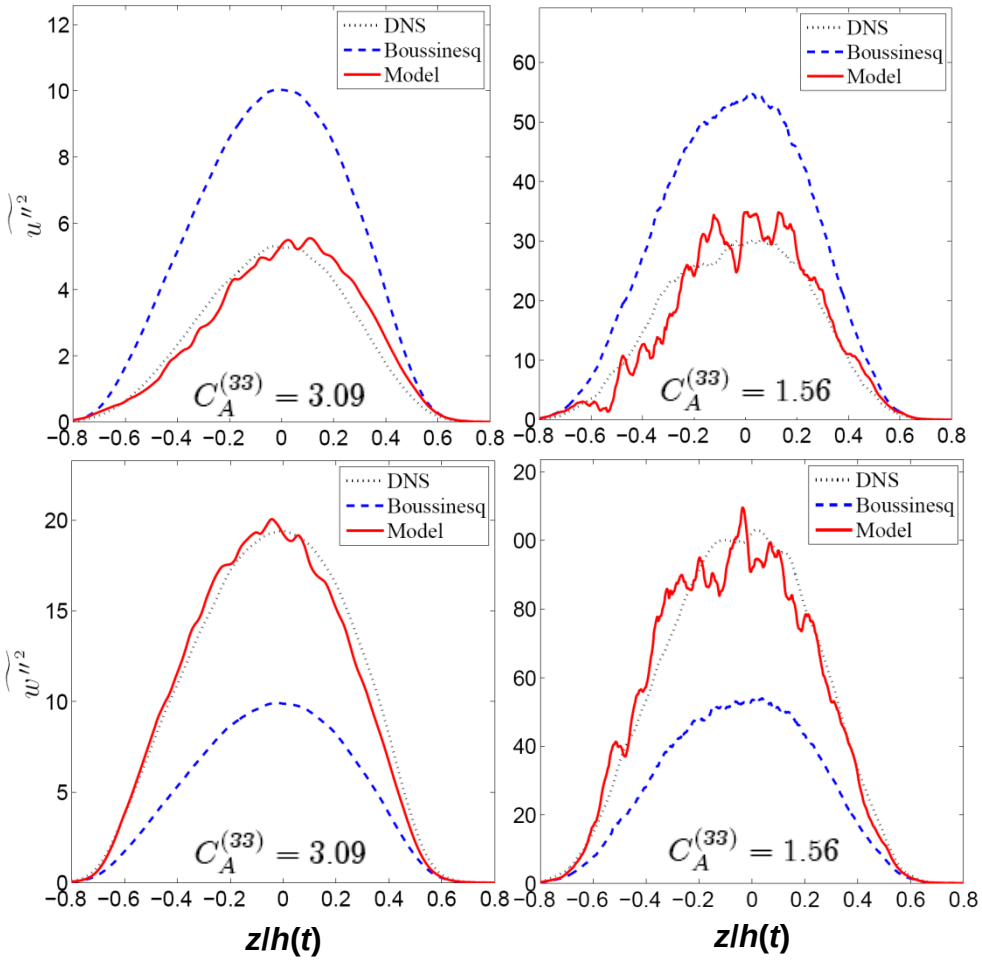

Gradient-diffusion models for the turbulent kinetic energy and energy dissipation fluxes generally agree well with DNS for $t/t_0 \geq 9$

- **Flux of turbulent kinetic energy and its dissipation rate**

$$\overline{\rho}\,\widetilde{E''w''} = -\frac{\mu_t}{\sigma_k}\frac{\partial \widetilde{E''}}{\partial z} \quad , \quad \overline{\rho}\,\widetilde{\epsilon''w''} = -\frac{\mu_t}{\sigma_\epsilon}\frac{\partial \widetilde{\epsilon''}}{\partial z}$$

- **Turbulent viscosity ($C_\mu = 0.09$)**

$$\nu_t = \frac{\mu_t}{\overline{\rho}} = C_\mu \frac{\left(\widetilde{E''}\right)^2}{\widetilde{\epsilon''}}$$

- **Better agreement on heavy side of mixing layer and at later times**

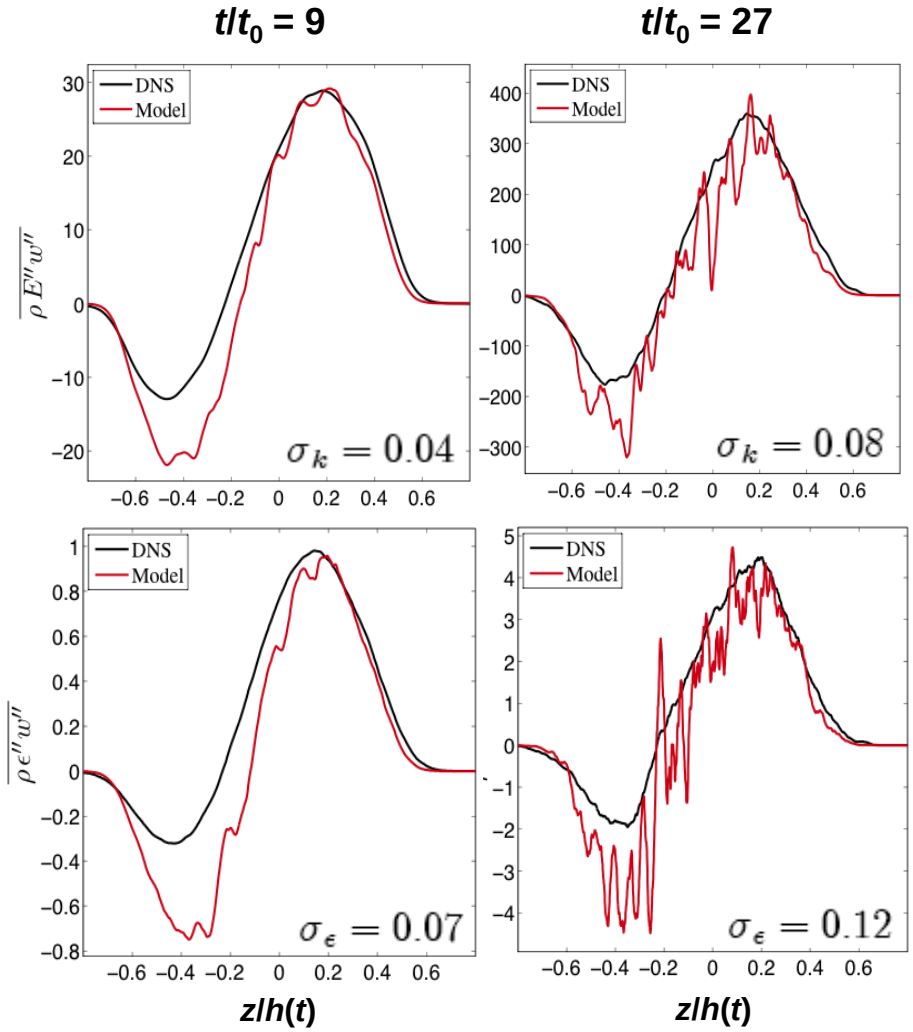

Gradient-diffusion models for the buoyancy and shear production of turbulent kinetic energy agree well with DNS at all times

- **Buoyancy and shear production of turbulent kinetic energy**

$$P_b^{\widetilde{E}''} = \frac{\overline{\rho' w'}}{\overline{\rho}} \frac{\partial \overline{p}}{\partial z} = -\frac{\nu_t}{\sigma_\rho \overline{\rho}} \frac{\partial \overline{\rho}}{\partial z} \frac{\partial \overline{p}}{\partial z}$$

$$P_s^{\widetilde{E}''} = -\tau_{ij} \frac{\partial \widetilde{u}_i}{\partial x_j}$$

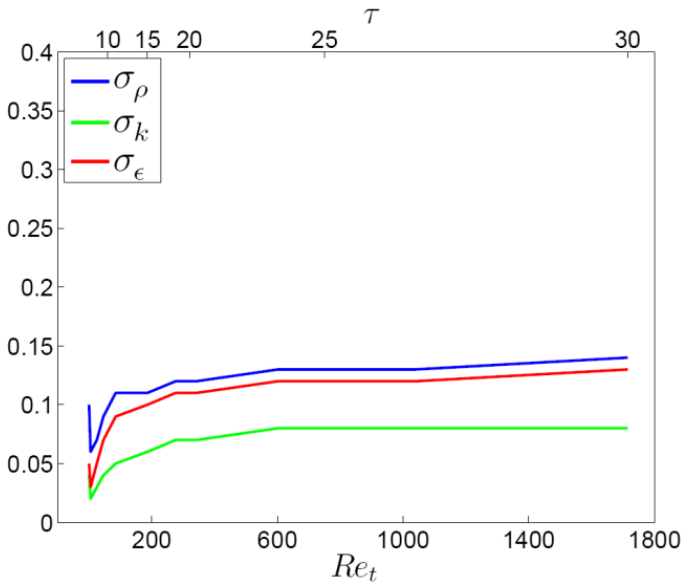

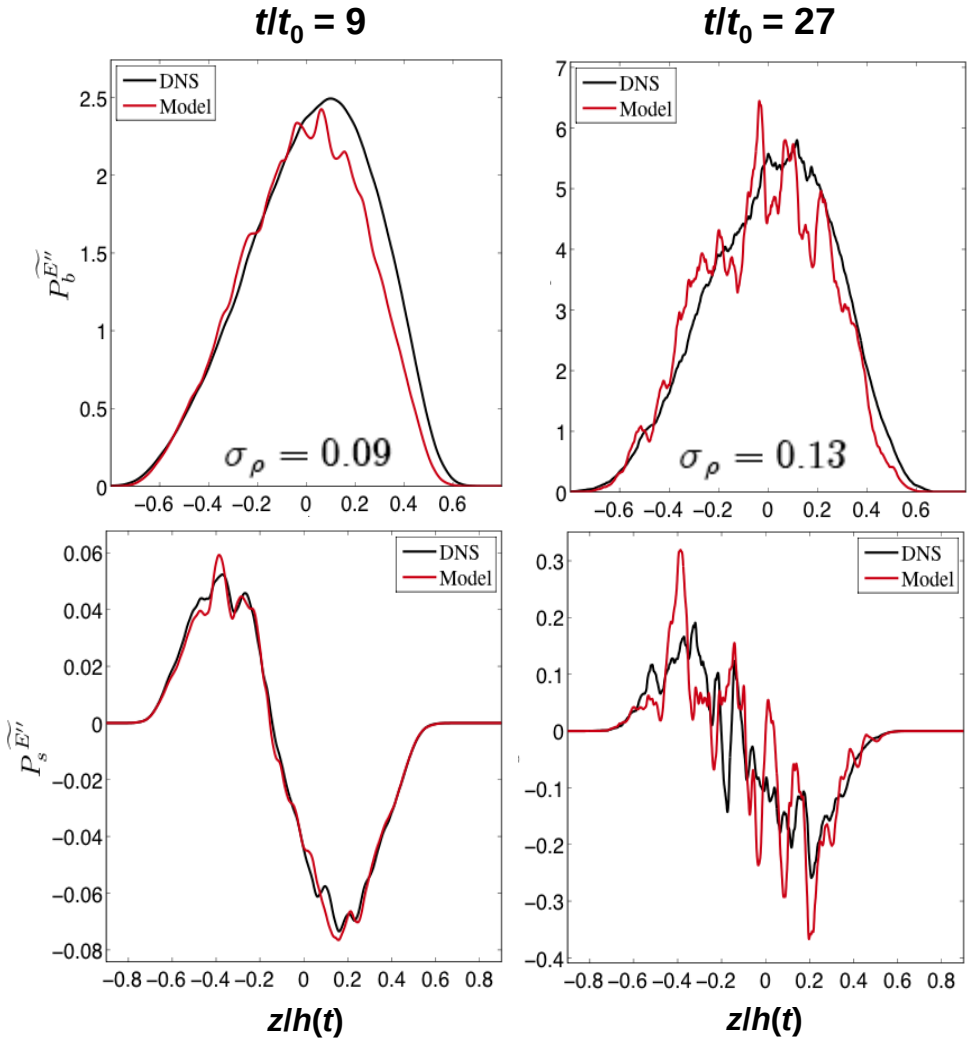

Gradient-diffusion models for the density variance and density variance dissipation rate flux exhibit good agreement with DNS for $t/t_0 \geq 9$

- **Flux of density variance and of its dissipation rate**

$$\overline{\rho'^2\, w''} = -\frac{\lambda_t}{\sigma_{\rho 2}} \frac{\partial}{\partial z}\left(\frac{\overline{\rho'^2}}{\overline{\rho}}\right) \quad , \quad \overline{\epsilon'_\rho\, w''} = -\frac{\lambda_t}{\sigma_{\epsilon\rho}} \frac{\partial \overline{\epsilon'_\rho}}{\partial z}$$

- **Turbulent diffusivity**

$$D_t = \frac{\lambda_t}{\overline{\rho}} = C_\mu \frac{2\,\overline{\rho'^2}\,\widetilde{E''}}{\overline{\epsilon'_\rho}}$$

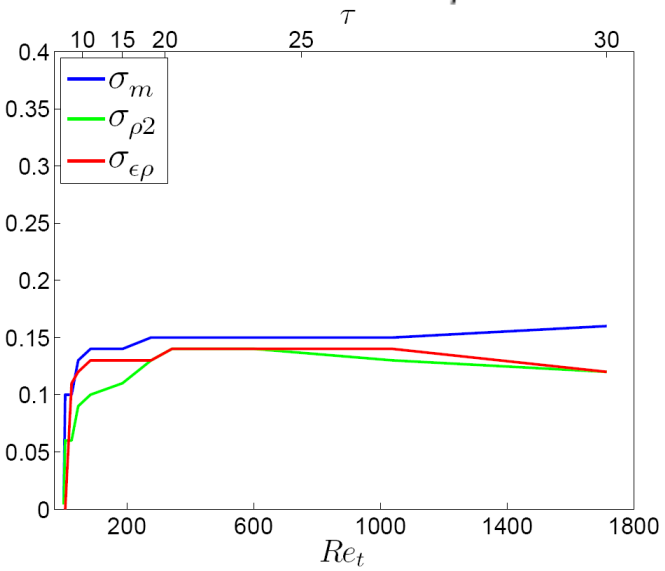

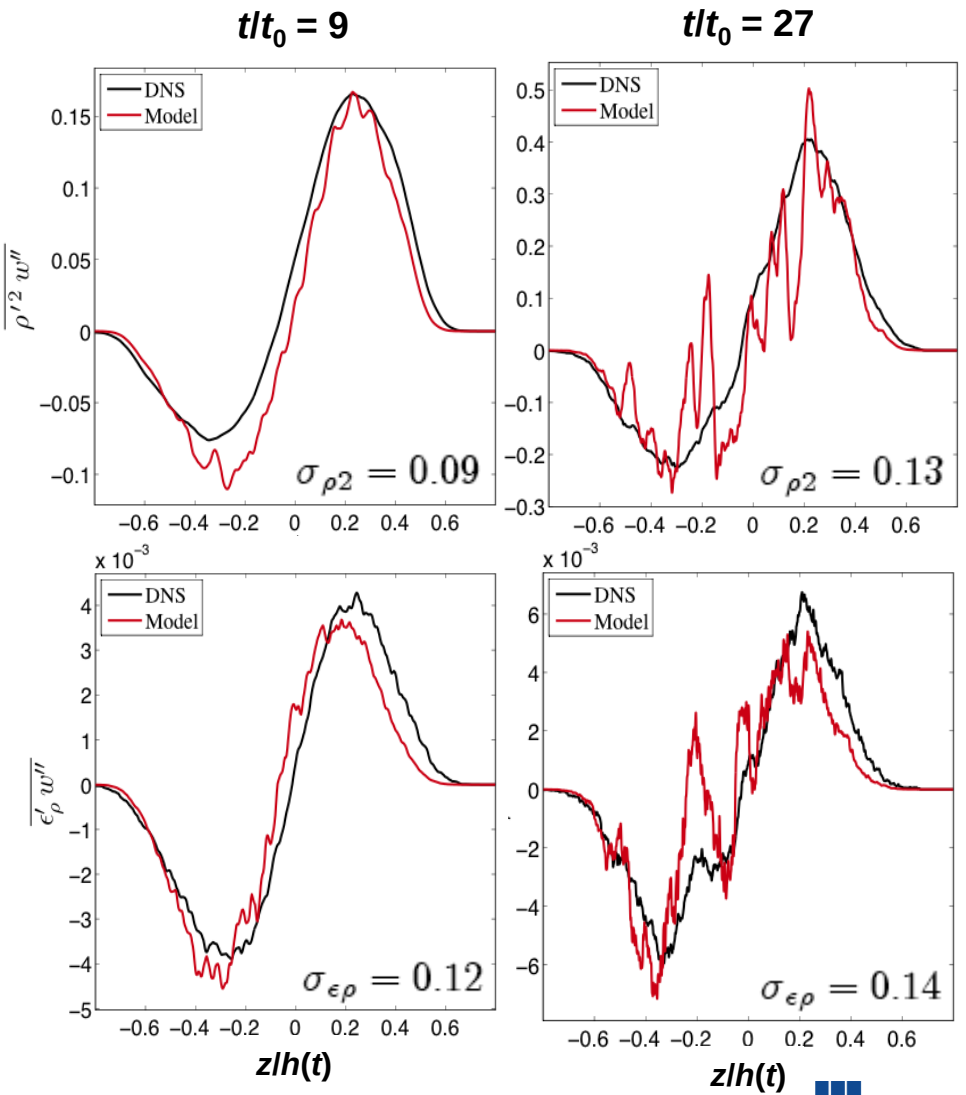

The buoyancy and shear production of turbulent kinetic energy dissipation rate exhibit very good agreement at all times

- **Buoyancy and shear production of turbulent kinetic energy dissipation rate**

$$P_b^{\widetilde{\epsilon''}} = -C_{\epsilon 0} \frac{\widetilde{\epsilon''}}{\widetilde{E''}} \frac{\nu_t}{\sigma_\rho \overline{\rho}} \frac{\partial \overline{\rho}}{\partial z} \frac{\partial \overline{p}}{\partial z}$$

$$P_s^{\widetilde{\epsilon''}} = -C_{\epsilon 1} \frac{\widetilde{\epsilon''}}{\widetilde{E''}} \tau_{ij} \frac{\partial \widetilde{u}_i}{\partial x_j}$$

- $C_{\varepsilon 0}$ considerably smaller than at lower Atwood and Reynolds numbers
- $C_{\varepsilon 1}$ considerably smaller than in shear flows (1.44)

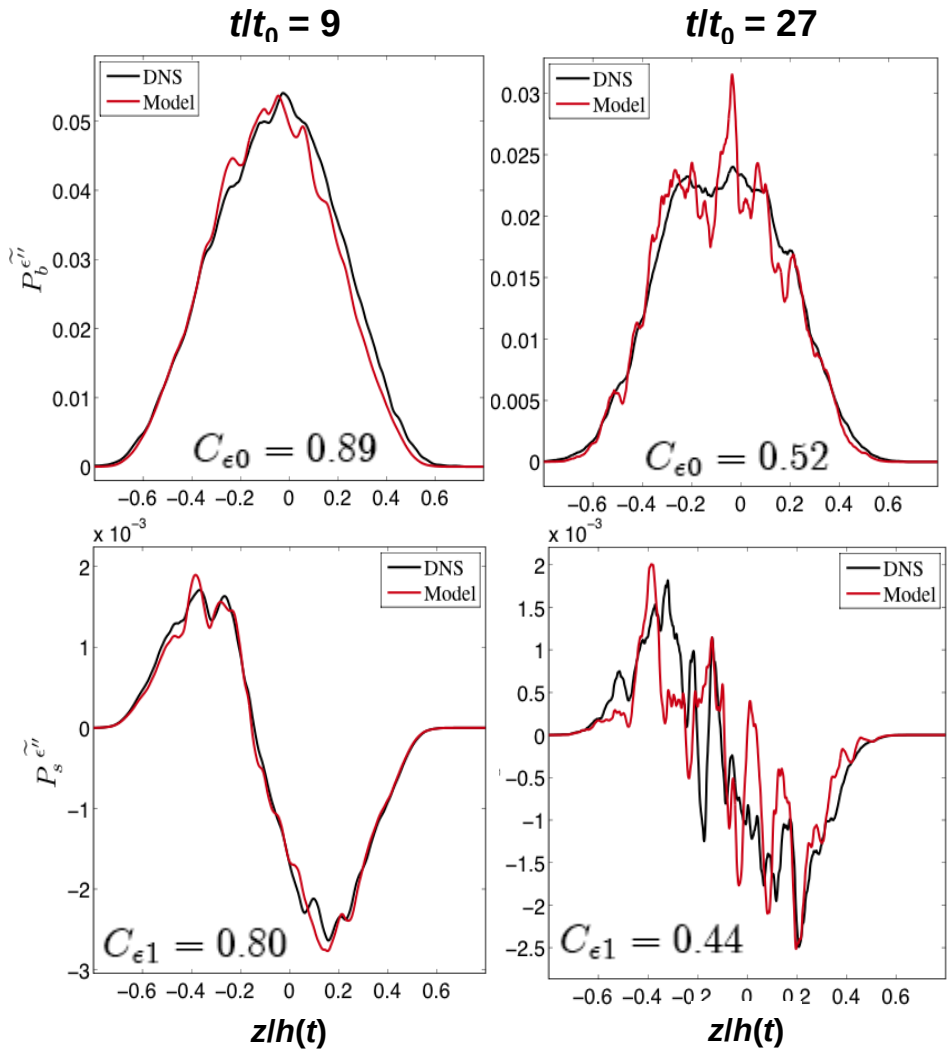

Order of magnitude estimates suggest modifications to the similarity models for turbulent production and destruction of ε

- **Turbulent production and destruction of turbulent kinetic energy dissipation rate**

$$P_t^{\widetilde{\epsilon''}} = C_{\epsilon 3}\sqrt{Re_t}\,\frac{\overline{\rho}\left(\widetilde{\epsilon''}\right)^2}{\widetilde{E''}} \quad , \quad D_t^{\widetilde{\epsilon''}} = C_{\epsilon 2}\sqrt{Re_t}\,\frac{\overline{\rho}\left(\widetilde{\epsilon''}\right)^2}{\widetilde{E''}}$$

- **Factors** $\sqrt{Re_t} = \sqrt{\left(\widetilde{E''}\right)^2 / \left(\widetilde{\epsilon''}\,\nu\right)}$ **arise from comparing order of magnitude estimate of exact and modeled terms**
- **Essential for "collapsing" coefficients**

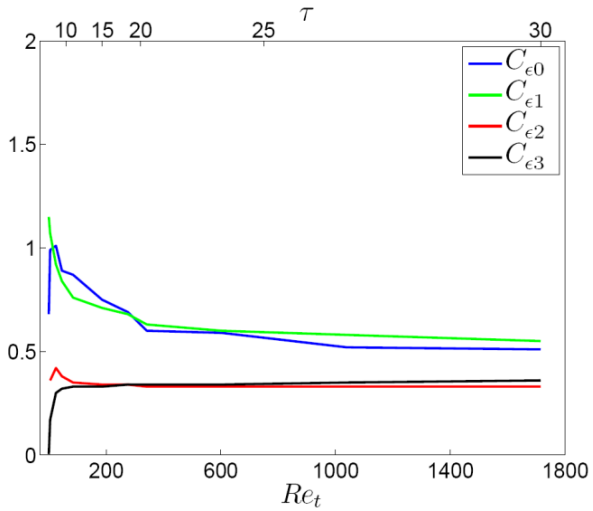

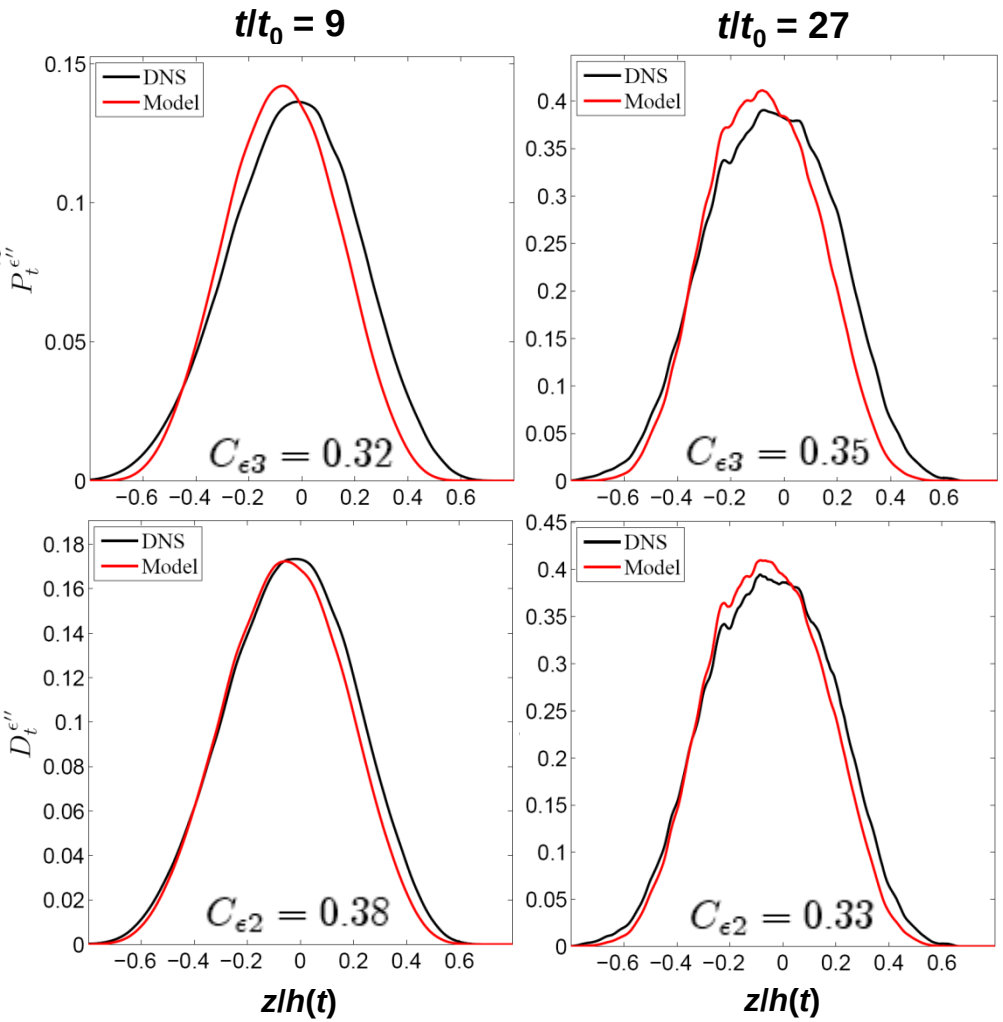

Algebraic models for the destruction of the density variance and density variance dissipation rate are in excellent agreement with DNS

- **Algebraic density variance dissipation rate and its destruction**

$$\overline{\epsilon'_\rho} = D\overline{\left(\frac{\partial \rho'}{\partial x_j}\right)^2} = C_{\rho 2}\frac{\widetilde{\epsilon''}}{\widetilde{E''}}\overline{\rho'^2}$$

$$D^{\overline{\epsilon'_\rho}} = 2\,D^2\overline{\left(\frac{\partial^2 \rho'}{\partial x_i \partial x_j}\right)^2} = C_{\epsilon\rho 2}\sqrt{Re_t}\,\overline{\epsilon'_\rho}\frac{\widetilde{\epsilon''}}{\widetilde{E''}}$$

- **Models accurately capture profile details at all times**
- **Accuracy of algebraic model suggests that a 3-equation model may be sufficient**

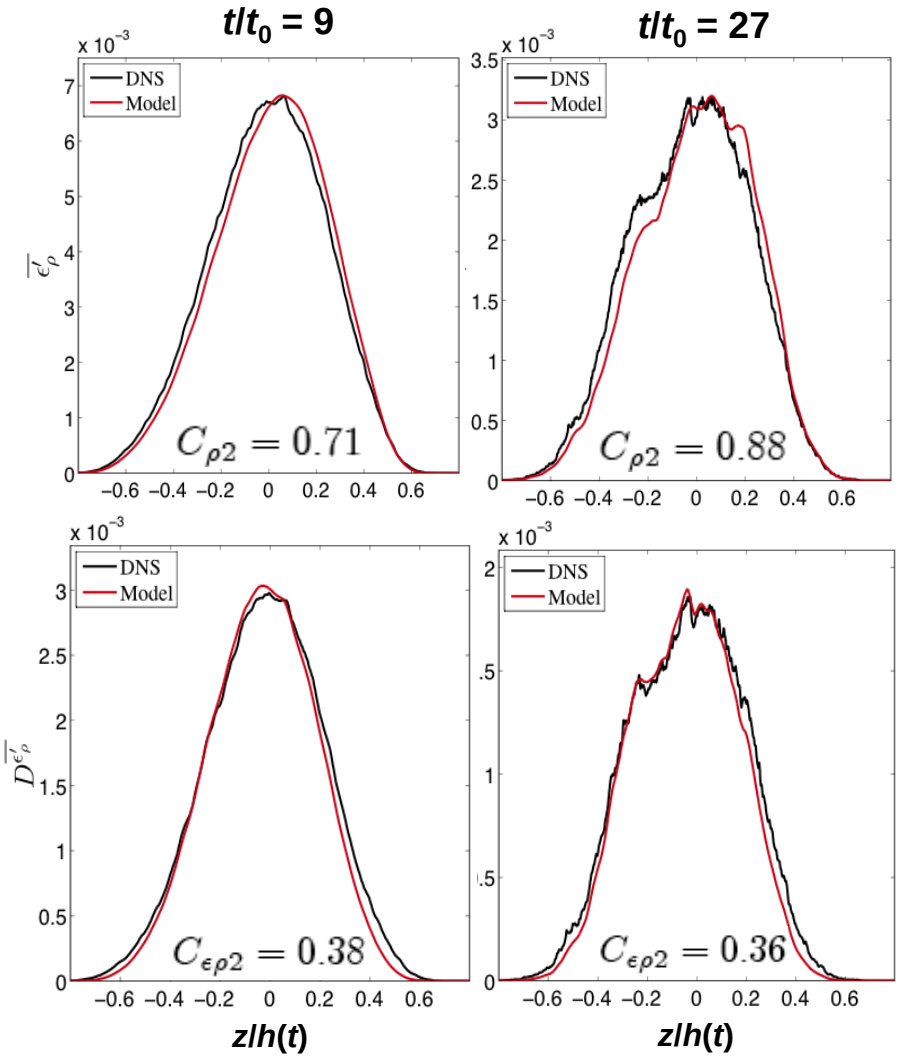

Similarity models for the mean and turbulent production of density variance dissipation rate exhibit good agreement at all times

- **Mean production of density variance dissipation rate**

$$P_m^{\overline{\epsilon'_\rho}} = -2\,D\,\overline{\frac{\partial \rho'}{\partial x_i}\frac{\partial u_j''}{\partial x_i}}\frac{\partial \overline{\rho}}{\partial x_j} = C_{\epsilon\rho 0}\frac{\nu_t}{\sqrt{Sc}}\frac{\overline{\epsilon'_\rho}}{\overline{\rho'^2}}\left(\frac{\partial \overline{\rho}}{\partial z}\right)^2$$

- **Turbulent production of density variance dissipation rate**

$$P_t^{\overline{\epsilon'_\rho}} = -2\,D\,\overline{\frac{\partial \rho'}{\partial x_i}\frac{\partial \rho'}{\partial x_j}\frac{\partial u_j''}{\partial x_i}} = C_{\epsilon\rho 3}\sqrt{Re_t}\,\frac{\left(\overline{\epsilon'_\rho}\right)^2}{\overline{\rho'^2}}$$

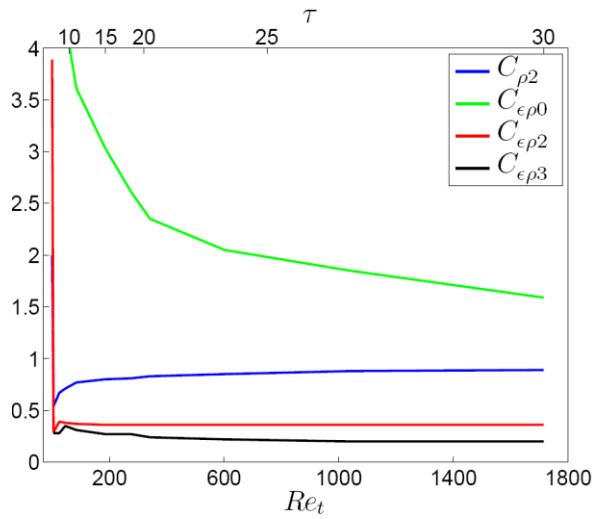

$t/t_0 = 9$ $t/t_0 = 27$

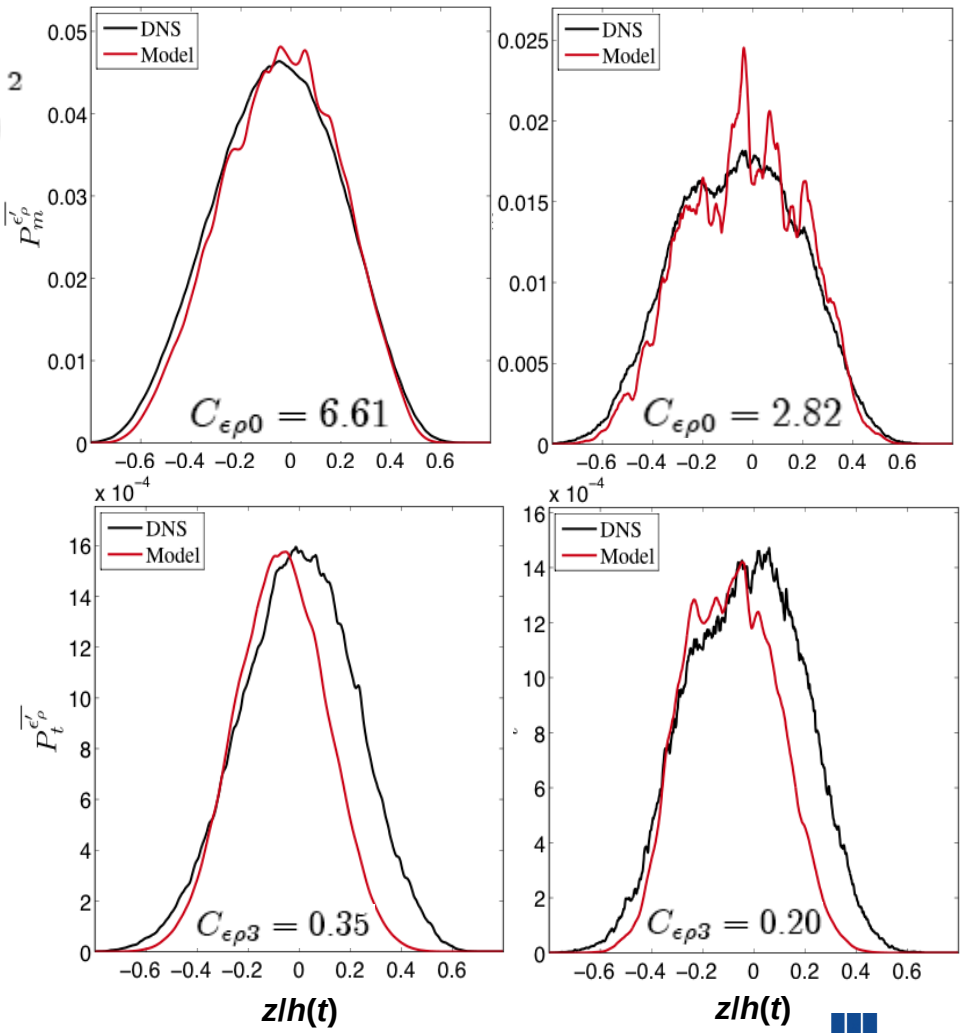

This work optimized gradient-diffusion and similarity models for Rayleigh–Taylor mixing and will be used to motivate improved RANS models

- **Gradient-diffusion and modified similarity models for second-order transport equations validated *a priori***
  - **Coefficients in optimized model computed using an L_2 minimization between DNS and model profiles**
  - ***Most* coefficients *nearly asymptote* in self-similar regime at late times**
- **Suggests a 4-equation RANS model (or 3-equation model with algebraic $\overline{\epsilon'_\rho}$):**

$$\overline{\rho}\left(\frac{\partial}{\partial t}+\widetilde{u}_j\frac{\partial}{\partial x_j}\right)\widetilde{E''}=-\frac{\nu_t}{\sigma_\rho\,\overline{\rho}}\frac{\partial\overline{\rho}}{\partial x_j}\frac{\partial\overline{p}}{\partial x_j}-\tau_{ij}\,\widetilde{S}_{ij}-\overline{\rho}\,\widetilde{\epsilon''}+\frac{\partial}{\partial x_j}\left(\frac{\mu_t}{\sigma_k}\frac{\partial\widetilde{E''}}{\partial x_j}\right)$$

$$\overline{\rho}\left(\frac{\partial}{\partial t}+\widetilde{u}_j\frac{\partial}{\partial x_j}\right)\widetilde{\epsilon''}=-C_{\epsilon 0}\frac{\widetilde{\epsilon''}}{\widetilde{E''}}\frac{\nu_t}{\sigma_\rho\,\overline{\rho}}\frac{\partial\overline{\rho}}{\partial x_j}\frac{\partial\overline{p}}{\partial x_j}-C_{\epsilon 1}\frac{\widetilde{\epsilon''}}{\widetilde{E''}}\tau_{ij}\,\widetilde{S}_{ij}+(C_{\epsilon 3}-C_{\epsilon 2})\sqrt{Re_t}\frac{\overline{\rho}\left(\widetilde{\epsilon''}\right)^2}{\widetilde{E''}}+\frac{\partial}{\partial x_j}\left(\frac{\mu_t}{\sigma_\epsilon}\frac{\partial\widetilde{\epsilon''}}{\partial x_j}\right)$$

$$\left(\frac{\partial}{\partial t}+\widetilde{u}_j\frac{\partial}{\partial x_j}\right)\overline{\rho'^2}=2\frac{D_t}{\sigma_\rho}\left(\frac{\partial\overline{\rho}}{\partial x_j}\right)^2-2\,\overline{\epsilon'_\rho}+\frac{\partial}{\partial x_j}\left[\frac{\lambda_t}{\sigma_{\rho 2}}\frac{\partial}{\partial x_j}\left(\frac{\overline{\rho'^2}}{\overline{\rho}}\right)\right]$$

$$\left(\frac{\partial}{\partial t}+\widetilde{u}_j\frac{\partial}{\partial x_j}\right)\overline{\epsilon'_\rho}=C_{\epsilon\rho 0}\frac{\nu_t}{\sqrt{Sc}}\frac{\overline{\epsilon'_\rho}}{\overline{\rho'^2}}\left(\frac{\partial\overline{\rho}}{\partial x_j}\right)^2+\sqrt{Re_t}\,\overline{\epsilon'_\rho}\left(C_{\epsilon\rho 3}\frac{\overline{\epsilon'_\rho}}{\overline{\rho'^2}}-C_{\epsilon\rho 2}\frac{\widetilde{\epsilon''}}{\widetilde{E''}}\right)+\frac{\partial}{\partial x_j}\left(\frac{D_t}{\sigma_{\epsilon\rho}}\frac{\partial\overline{\epsilon'_\rho}}{\partial x_j}\right)$$

Gradient-diffusion, modified similarity, and buoyancy-extended Reynolds stress models were validated for large *Re* Rayleigh–Taylor mixing†

- 3072^3 DNS; $At = 0.5$, $Sc = 1$; $Re = (h\, \mathrm{d}h/\mathrm{d}t)/\nu > 10^4$ at late time
- Early-time transient behavior is not generally captured by closures
- After transient and as flow begins to transition to self-similarity
  - Gradient-diffusion fluxes well reproduce DNS with nearly asymptotic coefficients
  - Similarity terms in dissipation rate equations modified by Re_t factors also well reproduce DNS with nearly asymptotic coefficients
- Buoyancy-extended Reynolds stress model motivated by ARSM closure in turbulent convection provides a reasonably good model compared to DNS

†Present work complements the BHR model study by D. Livescu et al., "High Reynolds number Rayleigh–Taylor turbulence," *Journal of Turbulence* 10, 13 (2009)

High-resolution DNS data has been used to develop and validate *a priori* 3- or 4-equation RANS models describing mechanical and scalar turbulence in Rayleigh–Taylor turbulent mixing